

Part I

HEAT TRANSFER COEFFICIENTS AND CORRECTIONS FOR THERMOCOUPLES IN
THE BOUNDARY LAYER OF A SPHERE

Part II

LOCAL CONVECTIVE HEAT TRANSFER FROM A SPHERE

Part III

THERMAL TRANSFER IN TURBULENT GAS STREAMS. EFFECT OF TURBULENCE
ON LOCAL TRANSPORT FROM SPHERES

Thesis by

Wallace Walter Short

IN Partial Fulfillment of the Requirements

For the Degree of

Doctor of Philosophy

California Institute of Technology

Pasadena, California

1958

ACKNOWLEDGMENT

The guidance of Professor B. H. Sage in my studies and research is gratefully acknowledged. The assistance and interest of H. E. Smith and R. A. S. Brown in pursuing the experimental work was invaluable. N. T. Hsu and K. Sato constructed much of the laboratory equipment and obtained some of the data used in this thesis. The reduction of the laboratory data was done by Lorine Faris. Virginia Berry prepared many of the figures and Evelyn Anderson typed the manuscript.

I am grateful to the Fluor Corporation for its financial support through the Peter E. Fluor Fellowship awarded me during 1955-57. The financial aid given by the Institute through scholarships and assistantships was most welcome.

ABSTRACTS

Part I

The deviation of thermocouple temperatures from the temperature of the fluid surrounding the junction as a result of conduction along the leads was studied. Measurements were made around a $\frac{1}{2}$ -inch heated sphere in the plane of the equator normal to an air stream whose velocity was 16 feet per second. Point air temperatures in the boundary layer of the sphere were predicted from the indications of a 0.001-inch diameter thermocouple with wires of platinum and platinum alloyed with 10% rhodium. The method employed also determined the heat transfer coefficients for the thermocouple wire in the boundary layer. These local heat transfer coefficients are lower than those observed in a uniform stream whose velocity is equal to the local velocity in the boundary layer.

Part II

The local convective heat transfer from a heated sphere 0.5 inch in diameter was determined by means of temperature gradients measured in the boundary layer. Point temperatures were obtained in the boundary layer with a 0.001-inch diameter thermocouple mounted on a probe. The sphere was suspended in air streams at velocities of 4, 8, 16, and 32 feet per second and at a turbulence level of 0.013. Local Nusselt numbers were computed for seven positions around the sphere at Reynolds numbers between 800 and 7000.

Part III

The present investigation was undertaken because of the absence of data concerning the effect of level of turbulence upon local thermal transport from spheres. A series of measurements was made of the local thermal transport in the forward hemisphere and a part of the after hemisphere of a silver sphere 0.5 inch in diameter. The measurements were made in an air stream the longitudinal turbulence level of which was varied between 0.013 and 0.146 for Reynolds numbers up to 3600.

At a turbulence level of 0.013 and a Reynolds number of 3600, the local heat transfer varied by a factor of seven around the sphere. Increasing the level of turbulence to 0.15 increased the over-all heat transfer 20 per cent. The local heat transfer varied by a factor of three at this high level of turbulence.

TABLE OF CONTENTS

PART	TITLE	PAGE
I	HEAT TRANSFER COEFFICIENTS AND CORRECTIONS FOR THERMO- COUPLES IN THE BOUNDARY LAYER OF A SPHERE	1
	Introduction	1
	Apparatus	3
	Analysis	4
	Experimental Procedure	20
	Discussion of Results	23
	Conclusions	27
	Nomenclature	28
	References	30
	Figures	32
	Tables	46
II	LOCAL CONVECTIVE HEAT TRANSFER FROM A SPHERE	54
	Introduction	55
	Analysis	57
	Methods and Equipment	60
	Experimental Results	62
	Discussion of Results	65
	Nomenclature	67
	References	68
	Figures	70
	Tables	76
III	THERMAL TRANSFER IN TURBULENT GAS STREAMS. EFFECT OF TURBULENCE ON LOCAL TRANSPORT FROM SPHERES	84
	Introduction	85
	Analysis	86
	Methods and Equipment	89
	Experimental Results	92
	Acknowledgment	96
	Nomenclature	97
	Literature Cited	98
	Figures	100
	Tables	106
	PROPOSITIONS	

Part I

HEAT TRANSFER COEFFICIENTS AND CORRECTIONS FOR THERMOCOUPLES IN
THE BOUNDARY LAYER OF A SPHERE

INTRODUCTION

Measurement of the local temperature of a fluid in the presence of large temperature gradients is a major experimental problem encountered in many heat transfer studies. The differential equations used to describe the temperature in and around temperature-sensing devices are usually simple, but the analytic solution to these equations is often impossible because of unusual geometry or irregular boundary conditions. Carslaw (1) and Ingersoll(2) present equations and a few solutions applicable to heat conduction problems faced when using thermocouples.

Several investigators have studied the problem of conduction in thermocouples. Johnson (3) determined analytically the thermocouple temperature for each of five air temperature distributions along the thermocouple leads. Boelter (4) corrected the readings of thermocouples mounted on flat plates in heaters. Hsu (5) presented an analog method for correcting thermocouple readings taken in the boundary layer surrounding a heated sphere. Extensive studies of corrections for hot wire anemometers were made by King (6). In many cases, King's results can be applied to thermocouples because of similar geometry and boundary conditions. The application of all these results presumes a knowledge of the heat transfer coefficient for the wire. The present study developed a method which does not require an independent knowledge of the heat transfer coefficient for predicting point air temperatures from the indications of small thermocouples.

A program designed to study the effect of free stream turbulence on the local thermal and material transfer from spheres was pursued in the Chemical Engineering Laboratory of the California Institute of Technology. In order to determine the local thermal flux from the surface of a sphere, point temperatures were measured in the fluid adjacent to the surface. For this purpose a thermocouple of small diameter was mounted on a probe, and temperature traverses were made with the thermocouple junction through the thermal boundary layer to the surface of the sphere. Traverse data of this type were presented by Hsu (5). Figure 1 presents junction temperatures from a typical experimental traverse. The term "junction temperature" is used here to distinguish the measured temperatures from the true "air temperature" at the same point in space. A third term "wire temperature" denotes temperatures in the thermocouple wire at points other than the junction. The term "thermocouple correction" will be used when referring to the difference between the air temperature and the junction temperature, i.e., $t_a - t_j$.

The position of the sphere-surface temperature in Figure 1 led earlier investigators to believe that the junction temperatures were considerably lower than the corresponding air temperatures and that thermal conduction along the thermocouple leads caused these deviations. This effect of conduction in the wire upon the junction temperature will be discussed in detail in this paper.

APPARATUS

A thermocouple made from platinum and platinum alloyed with 10% rhodium wires 0.001 inch in diameter was used in this investigation. The thermocouple was soldered to the tips of two needles on the probe. The dimensions of the thermocouple are shown in Figure 2. Wires 0.001 inch in diameter were chosen because this was the smallest size wire that could be butt welded in an oxy-natural gas flame to form a smooth cylindrical junction. No irregularities were observed at the junction under a 36-power binocular microscope. Thermocouples were made from 0.0003-inch diameter wires, but very irregular junctions resulted.

The probe and thermocouple could be moved parallel to each of the three coordinate axes shown in Figure 3. Dial indicators reading to 0.001 inch measured the displacement of the probe in the three axial directions. The thermocouple wires were always parallel to the y axis which was normal to the air stream.

The 0.5-inch sphere used in this investigation was employed in earlier studies of heat transfer from spheres by Sato (7). The surface of the sphere was formed by two silver hemispheres 0.016-inch thick fitted over a heated copper core. Four copper-constantan thermocouples were embedded in the inner surface of the silver shell to measure surface temperatures. The sphere was mounted on stainless steel tubes 0.096 inch in diameter provided with compensating heaters. When the heaters were properly adjusted, no heat was conducted to or from the sphere along the supports.

The air stream in which the sphere was suspended is described by Hsu (8) and by Corcoran (9). During the tests to be discussed, the air stream was maintained at a velocity of 16 feet per second, a temperature of 100°F and a turbulence level of 0.013. The turbulence level is the ratio of the root mean square of the lateral fluctuating velocity component divided by the average longitudinal velocity. The turbulence measurement was made by Sato using the method of Schubauer (10).

The wires from which the copper-constantan and probe thermocouples were made were calibrated in the laboratory. The laboratory calibrations, which differed slightly from data in the literature, were used to obtain all temperatures. Calibration of the platinum-platinum, 10% rhodium thermocouples gave results 0.5°F lower than the National Bureau of Standards reference tables for thermocouples (11) at 230°F. Calibration of the copper-constantan thermocouples gave temperatures 0.8°F lower than the tables at 230°F. The reference junction for all thermocouples was at the ice point.

ANALYSIS

This analysis of thermocouple corrections is divided into four sections. The contents of each section are as follows: (1) The assumptions made in the analysis are discussed in detail in the first section. (2) Considering only conductive and convective thermal transport, the differential equation describing temperature in the vicinity of the thermocouple is developed. The thermocouple correction is one

term in this equation. (3) The difficulties involved in evaluating each term in the differential equation are discussed. (4) Several particular solutions to the differential equation are found by means of a finite difference approximation. In these solutions wire temperatures are computed for an assumed air temperature distribution along the wire. The results of these computations indicate a method for obtaining air temperatures from junction temperatures, which is the objective of this investigation.

1. Assumptions

The temperature distribution normal to the axis of the wire is illustrated qualitatively in Figure 4. The temperature in the undisturbed air is shown as a dashed curve, while the temperature distribution with the thermocouple in place is shown by a solid curve. In this analysis it is assumed that the temperature within the wire is a function only of position in the y-direction. This assumption is the reason for the air temperature being shown equal on both sides of the wire in Figure 4.

Thermal transport by radiation from both the sphere and the thermocouple is small compared to the transport by convection. The total emissivity of the silver sphere, which was polished prior to testing, is 0.02 (12) at 212°F. The total emissivity of unoxidized platinum at 212°F is 0.047 (12). The emissivity of the wire surface near the junction is believed to be higher because it was oxidized in this area while welding the junction. Radiation transfer from an unoxidized platinum wire at 238.8°F, the maximum junction temperature observed experimentally, to the

surroundings at 80°F is $0.0035 \text{ Btu}/(\text{sq. ft.})(\text{sec.})$. The minimum heat transfer coefficient encountered in this investigation is $0.04 \text{ Btu}/(^{\circ}\text{F})(\text{sq. ft.})(\text{sec.})$. In order to transfer energy at a rate of $0.0035 \text{ Btu}/(\text{sq. ft.})(\text{sec.})$ from a body having this heat transfer coefficient requires a temperature difference of 0.09°F . Radiation may be responsible for a maximum thermocouple correction of this magnitude under the experimental conditions.

Uncertainty in the position of the thermocouple junction may be as large as ± 0.0005 inch in the z direction. An error of 0.0005 inch causes an error of 0.3°F in the junction temperature at the maximum gradient observed. This is a small error compared to the thermocouple correction of 12.28°F observed at the surface of the sphere. Errors less than 0.1°F are neglected in this study.

An ideal, stationary temperature-sensing element in a flowing stream indicates the stagnation temperature. The stagnation temperature is a measure of the kinetic energy and is estimated from the velocity and the heat capacity of the fluid. Theory predicts for a fluid in potential flow around a sphere a maximum velocity of 24 feet per second at the equator when in a stream having a velocity of 16 feet per second. The temperature rise upon stagnation in air moving at 24 feet per second is 0.048°F .

The effect of temperature jump and accommodation coefficient is not well understood, but some experimental work has been done in this field (13,14). Temperature jump is a temperature discontinuity at an interface,

usually associated with heat transfer at low pressures. The accommodation coefficient is the fractional extent to which molecules that strike a surface attain the energy corresponding to the temperature of the surface. Temperature jump and accommodation coefficient are discussed by Kennard (15), who presents the following empirical equation for the temperature jump in air at a wall where a temperature gradient exists normal to the wall:

$$\Delta t = 2.7 \ell \frac{\partial t_a}{\partial n} \quad (1)$$

The coefficient, 2.7, is a function of the accommodation coefficient and was determined experimentally by Smoluchowski (14). Large temperature jumps are observed when heat is transferred across the interface between a solid and a rarefied gas (16). The mean free path, ℓ , is large in the case of a rarefied gas. An appreciable temperature jump may also exist at atmospheric pressure, where the mean free path is small, in the presence of a high temperature gradient. The maximum temperature gradient encountered experimentally was 6×10^3 °F per inch. The temperature jump estimated from equation 1 is 0.041°F.

These three phenomena, radiation, stagnation temperature and temperature jump, are therefore neglected in the analysis.

The temperature difference between the inner and outer surfaces of the silver shell on the sphere is computed to be 0.008°F at the maximum thermal flux. The internal thermocouples were embedded in an isothermal

surface; therefore, errors due to conduction in these thermocouples are negligible. On the basis of these data temperature discrepancies between the internal thermocouple and the surface of the sphere are neglected. The difference between the surface temperature of the sphere as measured by the internal thermocouples and the temperature of the probe-thermocouple junction when in contact with the surface is considered to be the thermocouple correction at the surface.

The analysis of thermocouple corrections will be based upon the following assumptions some of which have been discussed in this section:

- a. The wire temperature is uniform in any plane perpendicular to the axis of the wire.
- b. The mechanisms of energy transfer are conduction and convection.
- c. The kinetic energy of the air stream can be neglected in the equation describing energy transport.
- d. Local equilibrium exists; i.e., there are no temperature discontinuities.
- e. The surface temperature of the sphere is measured by the internal thermocouples.
- f. The air temperature and velocity fields in the region investigated are symmetrical about the x axis.

2. Derivation of the Differential Equation

In order to determine the thermocouple correction at a point in the air stream, the differential equation describing the temperature in the vicinity of the wire is developed. The convective thermal transfer rate

per unit area results from the difference between the local air temperature and the wire temperature as indicated by equation 2.

$$\dot{Q} = h(t_a - t) \quad (2)$$

The energy transfer rate per unit length of wire is given by:

$$\dot{Q} = \pi h D (t_a - t) \quad (3)$$

The rate of energy loss per unit length of wire by conduction along the wire is

$$\dot{Q} = - \frac{\pi D^2}{4} \frac{d}{dy} \left(k \frac{dt}{dy} \right) \quad (4)$$

Under steady conditions, the energy gain from the stream may be equated to the loss by conduction in the wire. Combining equations 3 and 4 and simplifying, the following equation results:

$$t_a - t = - \frac{D}{4h} \frac{d}{dy} \left(k \frac{dt}{dy} \right) \quad (5)$$

Establishment of the air temperature from the junction temperature by means of equation 5 presents several difficulties.

3. Evaluation of Terms in the Differential Equation

The heat transfer coefficients obtained by Cole (17) are depicted in Figure 5 for 0.001-inch and 0.0003-inch wires in air. Using Frössling's theory (18) for the velocity distribution around a body of revolution, the data for a 0.001-inch wire are presented in Figure 6 as a function of radial distance from the sphere. The calculation of these theoretical air velocities are based on the assumption that laminar flow exists in the boundary layer and potential flow exists outside the boundary layer. Errors may be introduced by these assumptions; however, these heat transfer coefficients may be subject to other errors when applied to wires in a boundary layer, for reasons which will be discussed later.

The thermal conductivity of platinum is more than twice that of the platinum-rhodium alloy (19). The value to be substituted in equation 5 for the junction is not apparent. The evaluation of dt/dy near the junction or $k dt/dy$, the thermal flux through the junction, offers even greater problems. These factors require a knowledge of the wire temperature in the neighborhood of the junction, but only junction temperatures can be measured experimentally. The thermocouple junction can be moved a short distance along the axis of the wire on either side of the point to which equation 5 is being applied. In this way a temperature distribution in the neighborhood of the junction would be obtained. Moving the junction changes one boundary condition defining the solution to equation 5. This boundary condition is the thermal conductivity of the

wire as a function of y . Each junction temperature measured in this manner is one temperature from a different solution to the differential equation. The thermal flux, $k dt/dy$, established from these temperatures may be seriously in error.

To gain insight into this problem, it is assumed that the thermal conductivities of the metals in the thermocouple are constant and equal. Equation 5 then becomes

$$t_a - t = -\frac{Dk}{4h} \left(\frac{d^2 t}{dy^2} \right) \quad (6)$$

In this case the location of the junction is not one of the boundary conditions. The thermocouple is moved along its axis, and the wire temperatures remain constant with respect to the stationary coordinates. This applies to an infinite length of wire. For a finite length of wire it is assumed to be long enough to eliminate effects upon the region of interest caused by changes of end conditions. The second derivative of wire temperature and the thermal flux in the wire in this instance can be approximated from junction temperatures. The assumption of constant thermal conductivity throughout the wire permits the evaluation of all factors on the right side of equation 6 except the heat transfer coefficient. There are uncertainties in the heat transfer coefficients of Figure 6. The fact that the velocity and temperature fields are symmetrical about the x -axis is used to circumvent this problem.

Designate by 1 and 2, two points through which the thermocouple shown in Figure 3 may pass. Let these points be subject to the following conditions:

$$\begin{aligned}z_1 &> R \\z_2 &> R \\x_1 &= x_2 = 0 \\n_1 &= n_2\end{aligned}$$

Application of equation 6 to a wire at each point gives

$$t_{a_1} - t_1 = -\frac{Dk}{4h} \left(\frac{d^2t}{dy^2} \right)_1 \quad (7)$$

and

$$t_{a_2} - t_2 = -\frac{Dk}{4h} \left(\frac{d^2t}{dy^2} \right)_2 \quad (8)$$

Assumption f. in section 1 implies that

$$u_1 = u_2$$

and

$$t_{a_1} = t_{a_2} \quad (9)$$

By the additional assumption that the convective heat transfer coefficient for a wire at each point is solely a function of the local velocity, the following is true:

$$h_1 = h_2 \tag{10}$$

This is a valid assumption near the equator because the thermocouple is parallel to the y-axis and the local velocities are parallel to the x-axis. The flow is, therefore, normal to the thermocouple wire at all points. For points at $x \neq 0$ the flow is not necessarily parallel to the x-axis, and the heat transfer coefficient at a point depends on the orientation of the wire with respect to the flow. If equations 7, 8, 9, and 10 are solved for the air temperature at point 1 equation 11 is obtained.

$$t_{a,1} = \frac{t_1 - t_2 \frac{\left(\frac{d^2t}{dy^2}\right)_1}{\left(\frac{d^2t}{dy^2}\right)_2}}{1 - \frac{\left(\frac{d^2t}{dy^2}\right)_1}{\left(\frac{d^2t}{dy^2}\right)_2}} \tag{11}$$

Air temperatures can be computed from junction temperatures by means of equation 11, which is subject to the following restrictions:

$$h = f(n)$$

$$t_1 \neq t_2$$

$$k = \text{constant}$$

If an inflection point, i.e., $d^2t/dy^2 = 0$, occurs, it is obvious from equation 6 that the air temperature and junction temperature will be

identical at that point.

This analysis does not apply to a thermocouple containing a discontinuity in the thermal conductivity. It will be shown in the next section that the thermocouple correction at the inflection point of the junction-temperature curve obtained with a platinum, platinum alloy thermocouple is small. This is used to determine air temperatures experimentally.

4. Particular Solutions to the Differential Equations

In order to estimate the divergence of the thermocouple used in this investigation from the behavior described by equation 6, the wire temperature distributions in the probe thermocouple were computed as the junction moved along the axis of the wires through a known air-temperature field. If the thermocouple wire is divided by points called nodes which are Δy apart, a finite difference form of equation 5 is established in terms of these nodes.

$$(t_a)_n - t_n = -\frac{D}{4h_n\Delta y} \left[\frac{k_{n-1,n}(t_{n-1} - t_n)}{\Delta y} - \frac{k_{n,n+1}(t_n - t_{n+1})}{\Delta y} \right] \quad (12)$$

The subscript n designates the node to which this equation applies. Subscripts $n-1$ and $n+1$ refer to the adjacent nodes. This equation assumes that the thermal conductivity is uniform between nodes and the heat transfer rate to the air stream is uniform for a distance $\frac{1}{2}\Delta y$ on either side of node n . Letting the dimensionless quantities in equation 12 be

$$C_{n-1} = \frac{Dk_{n-1,n}}{4h_n\Delta y^2} \quad (13)$$

and

$$C_{n+1} = \frac{Dk_{n,n+1}}{4h_n\Delta y^2} \quad (14)$$

gives the following simplified form of equation 12:

$$-C_{n-1}t_{n-1} + (1 + C_{n-1} + C_{n+1})t_n - C_{n+1}t_{n+1} = (t_a)_n \quad (15)$$

If the wire contains $N + 1$ nodes, $n = 0, 1, \dots, N - 1, N$, a matrix of $N + 1$ equations can be written and solved for t at each node. The solution to the matrix is obtained by means of the following three equations:

$$P_n = \frac{C_{n+1}}{(1 + C_{n-1} + C_{n+1}) - C_{n-1}P_{n-1}} \quad (16)$$

$$Q_n = \frac{(t_a)_n + C_{n-1}Q_{n-1}}{(1 + C_{n-1} + C_{n+1}) - C_{n-1}P_{n-1}} \quad (17)$$

$$t_n = \rho_n t_{n+1} + q_n \quad (18)$$

when $t_{-1} = 0$ and $t_{N+1} = 0$.

A 31 node representation of the thermocouple in Figure 2 was solved in this fashion on a digital computer. The experimental junction temperature curve labeled $z = 0.256$ in Figure 8 was adjusted to make it symmetrical and used for the air temperatures in this analysis. The assumed air temperatures, normalized with respect to the maximum air temperature, are listed on the second page of Table I. The following data were also used:

- D = 0.001 inch
- Δy = 0.010 inch
- t_{-1} = 0
- t_{31} = 0
- h = 0.05 Btu/(°F)(sq.ft.)(sec.)
- k_{Pt} = 1.1416×10^{-2} Btu/(°F)(ft.)(sec.)
- k_{Rh} = 4.9133×10^{-3} Btu/(°F)(ft.)(sec.)

For the purpose of this calculation a typical value of 0.05 Btu/(°F)(sq.ft.)(sec.) for the heat transfer coefficient was chosen from Figure 6 and was considered uniform over the length of the wire. The thermal conductivities (19) of the metals at 212°F were used and also assumed uniform. The dimensionless quantities in equations 13 and 14 were determined for the two metals from the data above.

$$C_{Pt} = 6.850$$

$$C_{Rh} = 2.948$$

The wire temperature at each node was determined when the junction was at each of the 33 possible locations. The ends of the wire, $n = -1$ and $n = 31$, while not nodes, were considered possible locations of the junction. The results computed in these two cases were the wire temperatures in a homogeneous platinum wire and a homogeneous alloy wire. Thirty three independent solutions to the matrices were computed using the method outlined by equations 16, 17, and 18. Three solutions are shown in Table I. The differences between the air temperatures and wire temperatures, $t_a - t$, are listed in Table I rather than the wire temperature. The values of $t_a - t$ obtained at each node for the platinum and alloy wires are listed on the first page of Table I. The values of $t_a - t$ when the junction was at node 15, which coincided with the maximum air temperature, are listed on the second page of Table I. The thermocouple corrections, $t_a - t_j$, are also shown on this page opposite the node which the junction occupied. One value of $t_a - t_j$ was obtained from each of the 33 solutions. These are the only experimental data that would be measured by a thermocouple which is moved in 0.010-inch steps along its own axis through the assumed air temperature field. The data for the two homogeneous wires and the thermocouple corrections are plotted in Figure 7.

The second derivatives of temperature with respect to y for the three solutions presented in Table I are in the column following their respective values of $t_a - t$. The second derivatives of the junction

temperatures are also present. The second derivatives were approximated by the three-point method (20).

Several facts concerning the various temperature distributions are learned from the data of Table I. (a) The wire temperature at a point in the neighborhood of the junction is quite different than the temperature obtained from the junction at that point. (b) The point of maximum junction temperature does not coincide with the point of maximum air temperature. (c) The junction temperature at a particular point does not necessarily lie between the temperatures of the two homogeneous wires comprising the thermocouple. (d) The actual second derivative of wire temperature at a point may differ markedly from the value determined from junction temperatures. For example, the actual second derivative of wire temperature in the thermocouple presented in Table I is $236.8 \text{ }^\circ\text{F} / \text{in.}^2$ at node 16. The value obtained from junction temperatures is $195.7 \text{ }^\circ\text{F} / \text{in.}^2$. The disagreement of second derivatives obtained from junction temperatures and those obtained from wire temperatures rules out the use of junction temperatures as a means of solving equation 11. (e) The thermocouple correction at the inflection point in the junction-temperature data is small, but is not equal to zero.

This last statement does not eliminate the inflection point as a key to air temperatures. By interpolation of the data in Table I it is found that the junction temperatures at the inflection points differ by -0.020 and 0.017 from the air temperatures. These values are differences between normalized temperatures and, therefore, are fractions of the maximum

air temperature. Although small, 0.020 is four times the uncertainty of the experimental measurements. The maximum junction temperature is displaced +0.0013 inch from the maximum air temperature. If all junction temperatures are shifted 0.0013 inch in the minus y-direction the thermocouple corrections at the inflection points are 0.004 and 0.001. This is not an empirical adjustment of the data because the laboratory had to be handled in this manner. The point of maximum junction temperature in an experimental y-traverse was the only point available for establishing the y-coordinates of the junction temperatures relative to the sphere. Fixing the origin of the coordinates will be discussed in the section covering experimental procedure.

The locations of the thermocouple junction are believed to be measured within ± 0.0005 inch in the y-direction. For the air temperatures used in this analysis an error of ± 0.0005 inch in the y position of the junction would result in a ± 0.005 uncertainty in the normalized junction temperature at the inflection point. Only deviations in the y-direction are considered. Deviations in the z-directions may increase the uncertainty of the measured temperature. Errors of 0.004 in the normalized air temperatures are therefore within experimental accuracy. The junction temperature at the inflection point will be used to determine air temperature in the experimental study.

An "apparent thermal conductivity" of the junction was computed by substituting the second derivative of the computed wire temperatures in equation 6. The apparent thermal conductivity of the junction at the point of maximum junction temperature was 6.478×10^{-3} Btu/(°F)(ft)(sec).

This value lies between the thermal conductivities of platinum and the platinum with 10% rhodium alloy at 212°F, which are 11.416×10^{-3} Btu/(°F)(ft.)(sec.) and 4.9133×10^{-3} Btu/(°F)(ft.)(sec.) respectively.

EXPERIMENTAL PROCEDURE

Junction temperature curves were obtained from traverses made in the y-direction. All measurements reported here were made in the plane of the equator. The location of the equator of the sphere was determined in the laboratory by means of a cathetometer. The laboratory coordinates in the y and z-directions were based on the arbitrary datum positions of the dial indicators used. In order to transform these coordinates to coordinates whose origin was at the center of the sphere, y was set equal to zero at the maximum of the junction temperature curves. This may have introduced an error of approximately -0.001 inch in the true y-coordinate of each junction temperature, but this also led to the prediction of more accurate air temperatures at the inflection points. A traverse obtained along the z axis is shown in Figure 1. The point of contact between the thermocouple and the sphere was easily recognized on this curve as there was an abrupt change of slope at this point. The point of contact was at $z = 0.250$, the radius of the sphere. All coordinates are expressed in inches. This gave a relationship between the laboratory measurements in the z-direction and the z-coordinates relative to the center of the sphere. The data obtained from y-traverses are recorded as a function of the sphere coordinates in Table II and are plotted in Figure 8. The data at $z > 0.168$ in Figure 1 and the curve

$z = 0.248$ in Figure 8 were obtained by bending the wire over the sphere. The slight increase in thermocouple temperature in Figure 1 after touching the sphere was caused by lowering of the thermal resistance between the wire and sphere as the wire was pressed around the sphere.

Junction temperatures less than 100°F as indicated at $y = -0.120$ in Figure 8 were impossible because the air stream was maintained at 100°F . The y -traverses were limited at approximately $y = -0.120$ by a probe tip touching the sphere. It is believed that a very large temperature gradient existed across the solder attaching the thermocouple wire to the probe tip while the tip was in contact with the hot sphere. Under these conditions the solder-platinum alloy junctions generated an e.m.f. The e.m.f. was opposed to that of the thermocouple and resulted in an indication of a temperature less than 100°F .

The second derivatives of junction temperature with respect to y were computed using a three-point approximation (20) and are listed in Table III. The values of the second derivatives in the region $0.250 < z < 0.258$, $-0.05 < y < 0.05$ were scattered, but lay between $+19,000^{\circ}\text{F}/\text{in.}^2$ and $-25,000^{\circ}\text{F}/\text{in.}^2$ giving a flat appearance to the curves in this region. The portions of the curves in this region were omitted from Figure 9 to avoid confusion. Several steps were taken to obtain consistent curves; however, the second derivatives were extremely sensitive to minor adjustments of the data. The traverses were made in the y -direction in order to measure in as short a time interval as possible the three temperatures required to determine a second derivative. This reduced the effect

of drift in experimental conditions upon the second derivative. The temperatures, which were nearly linear with respect to z over a large portion of the field, were smoothed graphically on a t vs. z plot. No method of smoothing the data in the y direction was found which would give a consistent set of second derivatives. A five-point approximation (20) of the second derivative was tried, but it was found that using fewer points gave smoother results. The inflection points were estimated from Figure 9 and plotted as a single curve in Figure 8. A dashed line in Figure 9 shows the distribution of the second derivatives computed in the analysis.

Points of equal radial distance from the sphere are plotted as dashed lines in Figure 8. The intersection of each constant-radius curves with the inflection curve determined the air temperature at that radius. The two air temperatures determined at each radius are listed in Table IV. The arithmetic average of the two air temperatures is plotted in Figure 10. The thermocouple corrections at $y = 0$ are listed in Table IV and plotted in Figure 11. The inflection curve of Figure 8 did not approach the sphere closer than 0.014 inch; therefore, the air temperature and consequently the thermocouple correction could not be established in the region $0 < n < 0.014$. The thermocouple correction curve was ^xextrapolated through this region to the correction at the surface. Corrections computed by the method of Hsu (5) are shown in Figure 11 for comparison.

Heat transfer coefficients for the thermocouple wire were computed

using equation 6. The apparent thermal conductivity of the junction was used. The number of heat transfer coefficients that could be computed was limited to five because the thermocouple correction and the second derivative were known coincidentally at only five points. The heat transfer coefficients established by equation 6 are compared with those obtained from Cole (17) and Frössling (18) in Figure 12.

DISCUSSION OF RESULTS

The measured junction-temperature gradient normal to the sphere at the equator is 5730°F per inch under the conditions of this test. This value is the slope of the junction temperature curve in Figure 9 in the range $0 < n < 0.012$. The air-temperature gradient over the same range is 6010°F/in. The local thermal flux established from the junction temperatures would be 4.9% low in this instance. It is expected that the error in the local thermal flux determined in this manner will vary with position around the sphere because the thermocouple correction at the surface observed in other heat transfer studies (21) decreased with increasing polar angle. The polar angle is the angle at the center of the sphere between the forward stagnation point and the point in question. It is desired to develop thermocouple correction curves similar to Figure 11 that can be applied to all junction temperature traverses obtained around spheres. This will permit the calculation of the correct local thermal flux without repeating for each traverse the procedure described in this paper.

The thermocouple corrections in Figure 11 were normalized with respect

to the correction at the surface to obtain the values shown in Figure 13. The radial distances were normalized with respect to the thermal boundary layer thickness. The thermal boundary layer thickness, δ_t , computed from equation 19 was 0.0125 inch.

$$\delta_t = \int_0^{\infty} \frac{t_a - t_{\infty}}{t_s - t_{\infty}} dn \quad (19)$$

For a fluid with constant physical properties the normalized correction may be a function of one or more of the following parameters: free stream velocity, free stream turbulence, diameter of sphere, and polar angle. It is believed that the only effect of temperature is on the physical properties of the fluid. Hsu (21) related temperatures in the boundary layer of a sphere to the Blasius function (22). Curves of normalized air temperature as a function of normalized radial distance were presented which were nearly independent of the air stream velocity and polar angle. Likewise, the variation of the normalized correction with respect to these parameters may be small so the curve in Figure 13 would be applicable to other flow conditions. This will have to be established by further tests.

The large differences between the heat transfer coefficients found in this investigation and those of Cole (17) as shown in Figure 12 are not surprising. The resistance to thermal transfer by the fluid film on a wire in a field of high temperature and velocity gradients is not

adequately described by a heat transfer coefficient which is a function of velocity alone. The velocity gradient in the stream flowing normal to the wire produces pressure gradients in the boundary layer of the wire. Flow parallel to the axis of the wire will develop near the surface of the wire. If the thermal transport along this path by convection were comparable to that in the wire by conduction, the dimensionless term, C , computed in the analysis would be less than the correct value. Energy transfer in this manner may explain the flat appearance of the experimental second derivative curves in Figure 10 in the region near the surface of the sphere.

The slightly different than normal definition of air temperature used in equation 2 may also contribute to the disagreement of the heat transfer coefficients. Heat transfer coefficients are generally computed from the temperature difference between a solid body and the free stream at a distance from the body. The air temperature in equation 2 is defined as the temperature at the point in space where the wire temperature is obtained, when the wire is absent. This is demonstrated in Figure 4. The air temperature, while the wire is present and heat transfer is proceeding, does not exist. This distinction is only of consequence when high temperature gradients surround the wire.

The dashed portions of the curve in Figure 12 are estimated. It is possible that a definite minimum in the heat transfer coefficient exists near the surface. At a point in the low velocity fluid near the surface, the thermal transfer from the wire may be less than in regions of higher velocity or when the wire is in contact with the metal sphere.

The five values computed indicate that the thermal transfer is impeded by the presence of the sphere at a distance greater than predicted by the velocity distribution of Frössling.

Consider the thermal boundary layer, λ_t , to extend to a point at which the temperature is 99% of its free stream value. This new definition of the boundary layer thickness should not be confused with that of equation 19. The extent of the velocity boundary layer, λ_u , is the point at which the velocity determined by Frössling is 99% of that found in potential flow at the surface. The thicknesses of the thermal and velocity boundary layers according to this new definition are 0.0345 inch and 0.0141 inch, respectively. The heat transfer coefficient continues to increase outside the velocity boundary layer and appears to approach the free stream value near the limit of the thermal boundary layer. The air-temperature gradient may affect the heat transfer coefficient as has been suggested. A more likely explanation is that the velocity has not reached 99% of that in potential flow at 0.0141, but continues to increase in the region between 0.0141 inch and 0.0345 inch from the surface of the sphere. In this event the theory presented by Frössling does not adequately describe the boundary flow on a sphere. This result should be viewed in light of the difficulties involved in defining and studying heat transfer coefficients in high velocity and temperature gradients.

CONCLUSIONS

1. Heat transfer coefficients and thermocouple corrections can be obtained independently in the boundary layer on a sphere. Whether the results obtained in this investigation around a $\frac{1}{2}$ -inch sphere in an air stream whose velocity is 16 feet per second can be applied to other velocities and sphere diameters is not known.
2. The velocity boundary layer on a sphere appears to be thicker than predicted by Frössling (18).
3. Heat transfer coefficients in general are of limited utility when extrapolated to regions of high velocity and temperature gradients. Precise solutions to heat transfer problems in such a region require a rigorous solution to the equations of motion.

NOMENCLATURE

C	dimensionless group $Dk/\Delta h\Delta y^2$
d	differential operator
D	wire diameter, inch
f	a function
h	heat transfer coefficient, $\text{Btu}/(^{\circ}\text{F})(\text{sq. ft.})(\text{sec.})$
k	thermal conductivity, $\text{Btu}/(^{\circ}\text{F})(\text{ft.})(\text{sec.})$
l	mean free path
n	radial distance from surface of sphere, inch
\dot{Q}	specific thermal flux, $\text{Btu}/(\text{sec.})(\text{sq. ft.})$
\dot{Q}	thermal transfer rate per unit length, $\text{Btu}/(\text{sec.})(\text{ft.})$
R	radius of sphere, 0.250 inch
t	wire temperature, $^{\circ}\text{F}$
t_a	air temperature, $^{\circ}\text{F}$
t_j	junction temperature, $^{\circ}\text{F}$
Δt	temperature jump, $^{\circ}\text{F}$
U_{∞}	stream velocity
u	local velocity
x	coordinate axis, inch
y	coordinate axis, inch
z	coordinate axis, inch
δ	displacement boundary layer thickness defined by equation 17
λ	boundary layer thickness to 99% of free stream value
Δ	finite increment

Subscripts

n node
Pt platinum
Rh platinum alloyed with 10% rhodium
s surface of sphere
t temperature
u velocity
1 point in the air stream
2 point in the air stream
 ∞ free stream

REFERENCES

1. Carslaw, H. S., and Jaeger, J. C., "Conduction of Heat in Solids," Oxford Press, New York, 1947.
2. Ingersoll, L. R., Zobel, O. J., and Ingersoll, A. C., "Heat Conduction," McGraw-Hill Book Co., New York 1948.
3. Johnson, N. R., and Osterle, F., ASME Paper No. 57-HT-18, (1957).
4. Boelter, L. M. K., and Lockhart, R. W., NACA TN 2427 (1951).
5. Hsu, N. T., Calif. Inst. of Tech., thesis (1956).
6. King, L. V., Trans. Royal Soc. London, A 214, 373-432 (1914).
7. Sato, K., and Sage, B. H., ASME Paper no. 57-A-20 (1957).
8. Hsu, N. T., Reamer, H. H., and Sage, B. H., Document 4219, Am. Doc. Inst., Lib. of Congress, Washington, D. C. (1954).
9. Corcoran, W. H., Page, F., Schlinger, W. G., and Sage, B. H., Ind. Eng. Chem., 44, 410 (1952).
10. Schubauer, G. B., NACA Report No. 524 (1935).
11. Shenker, H., Lauritzen, J. I., Corruccini, R. J., and Lonberger, S. T., "Reference Tables for Thermocouples," Nat. Bur. of Std. Circ. 561 (1955).
12. Handbook of Chem. and Phy., 2199 (1945).
13. Dickins, B. G., Proc. Royal Soc. of London, A 143, 517 (1934).
14. Smoluchowski, M., Ann. Physik, 64, 101-130 (1898).
15. Kennard, E. H., "Kinetic Theory of Gases," McGraw-Hill Book Co., New York, pp. 149 & 311, 1938.
16. Eberly, D. K., Report No. HE 150-140, Univ. of Calif. Berkeley (1957).
17. Cole, J., and Roshko, A., Heat Transfer and Fluid Mech. Inst., 13-23 (1954).
18. Frossling, N., NACA TM 1432 (1953); english translation of: Frossling, N., Lunds Univ. Arsskrift, N. F. Ard. 2.36 No. 4 (1940).

19. International Critical Tables, V, 226 (1929).
20. Southwell, R. V., "Relaxation Methods in Theoretical Physics," Oxford Univ. Press, New York p. 17, 1946.
21. Hsu, W. T., and Sage, B. H., A.I.Ch.E. Journal, 3, 405-410 (1957).
22. Blasius, H., Z. angew. Math. Phys., 56, 1 (1908).

LIST OF FIGURES

1. Typical Junction-Temperature Traverse
2. Outline Drawing of Probe Thermocouple
3. Orientation of Probe Thermocouple and Sphere
4. Estimated Temperature Distribution around Wire
5. Convective Thermal Transport Coefficients for Small Wires in Air (17)
6. Convective Heat Transfer Coefficients for 0.001-Inch Diameter Wire near a 0.5-Inch Sphere (17,18)
7. Normalized Temperature Difference between Wire and Air
8. Experimental Junction Temperatures in Plane of Equator
9. Second Derivative of Experimental Junction Temperatures
10. Radial Temperature Distribution at Equator
11. Conduction Corrections for a 0.001-Inch Diameter Thermocouple
12. Experimental Convective Heat Transfer Coefficients for 0.001-Inch Diameter Wire near a 0.5-Inch Sphere
13. Dimensionless Conduction Corrections for a 0.001-Inch Diameter Wire

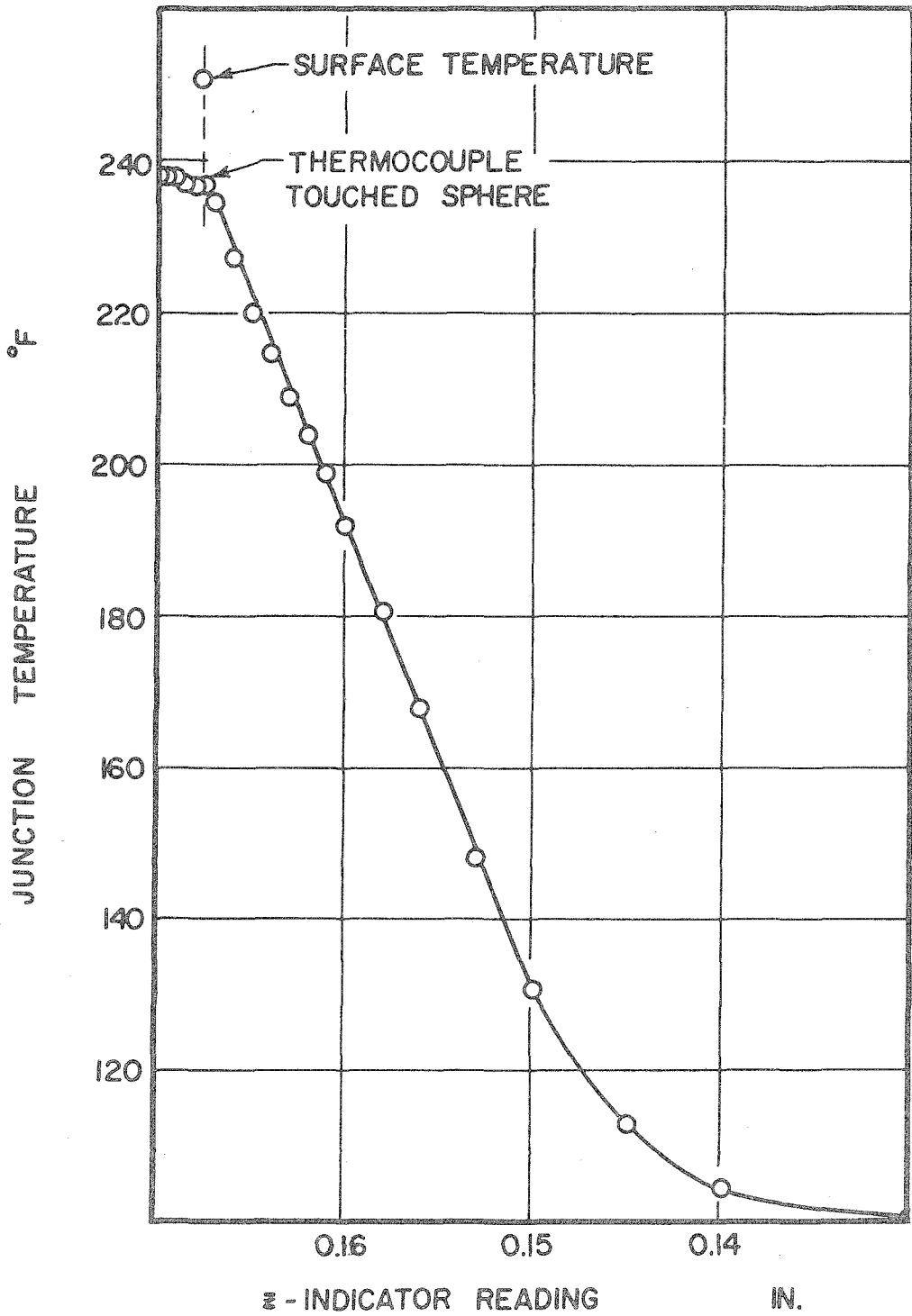


Fig. 1 Typical Junction-Temperature Traverse

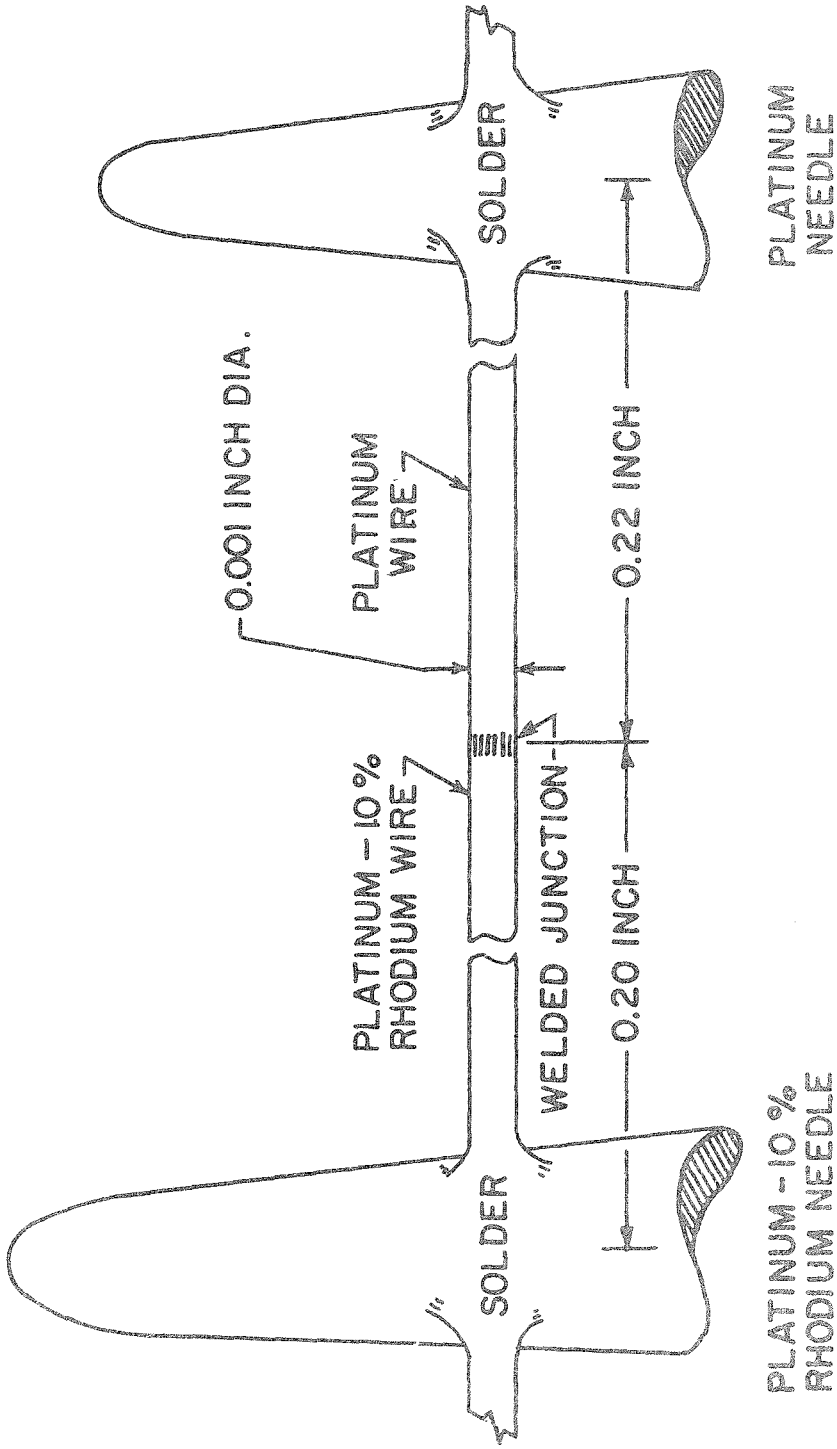


Fig. 2 Outline Drawing of Probe Thermocouple

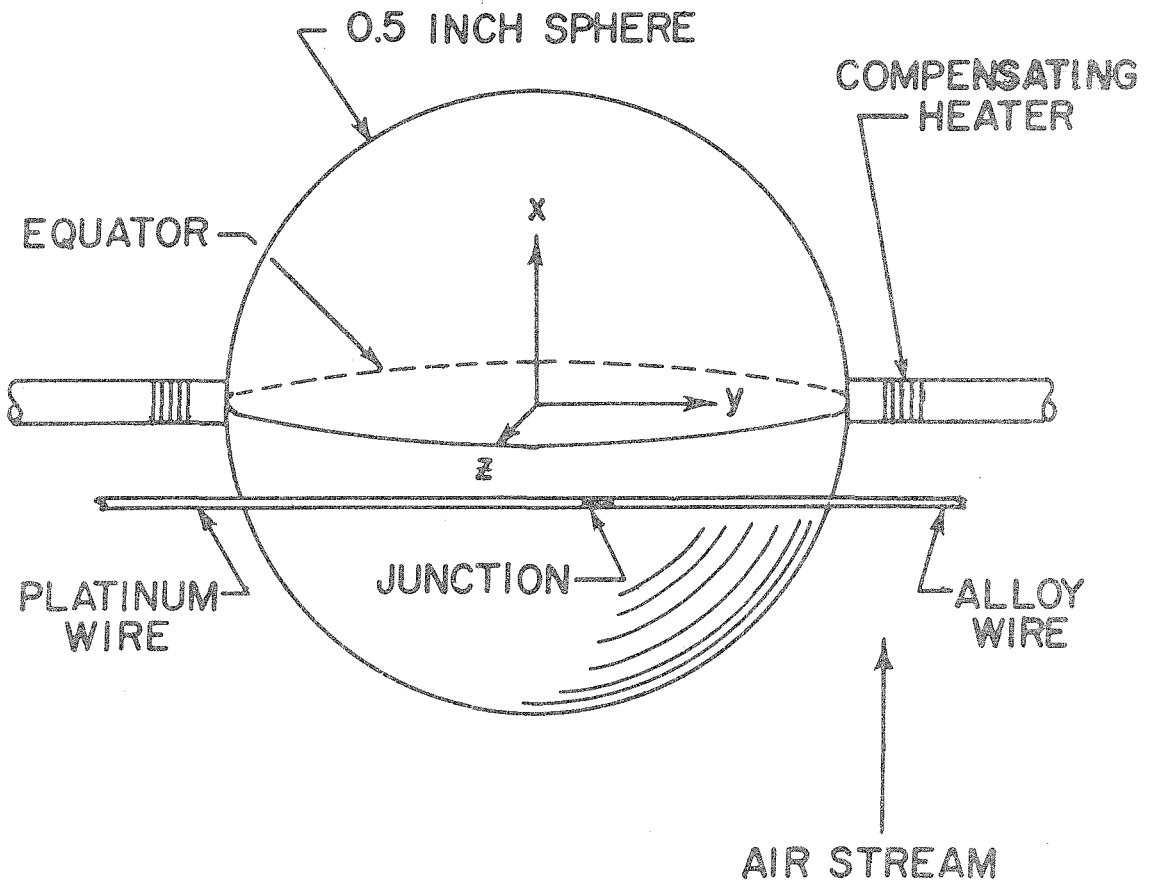


Fig. 3 Orientation of Probe Thermocouple and Sphere

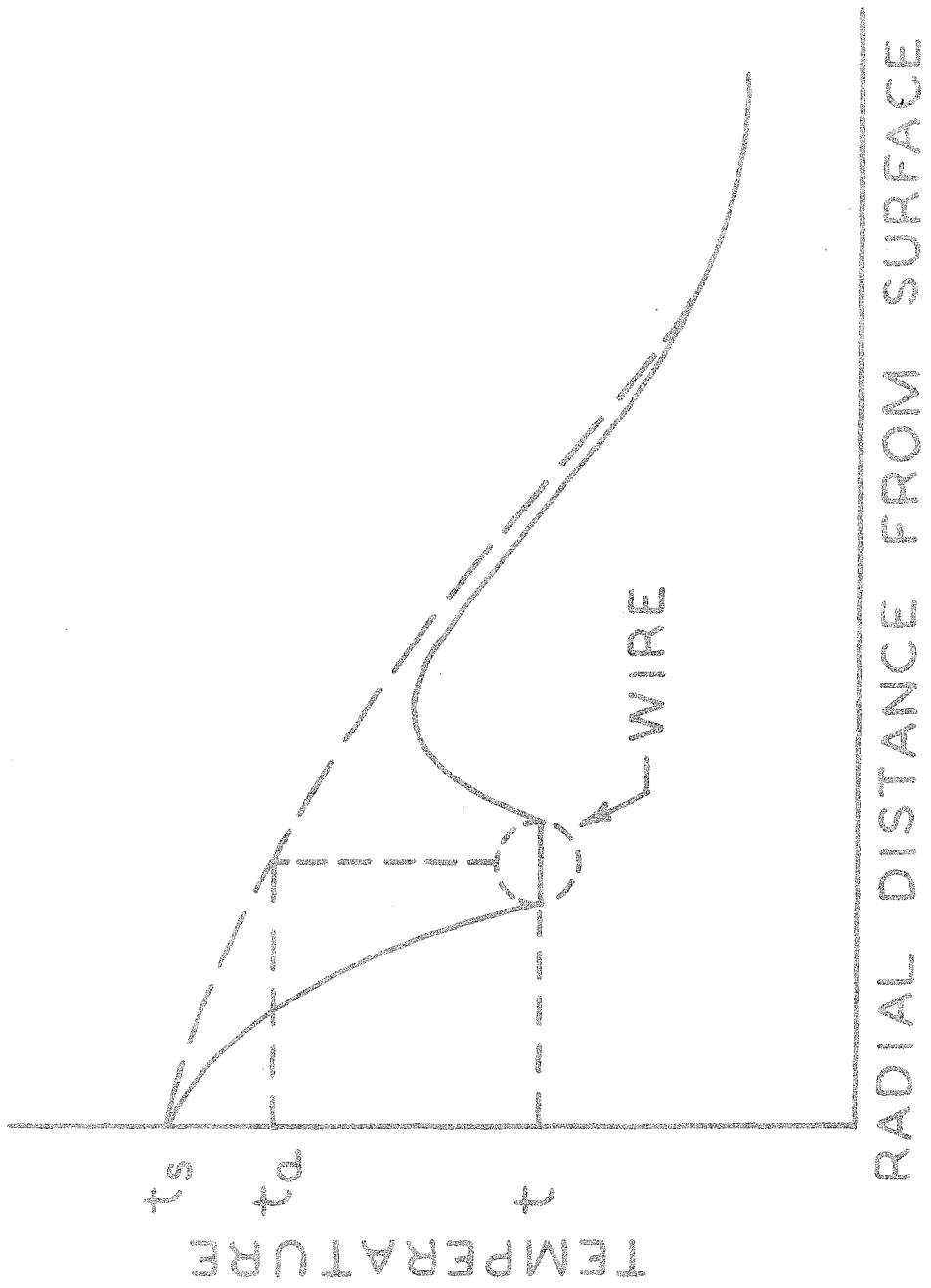


Fig. 4 Estimated Temperature Distribution around Wire

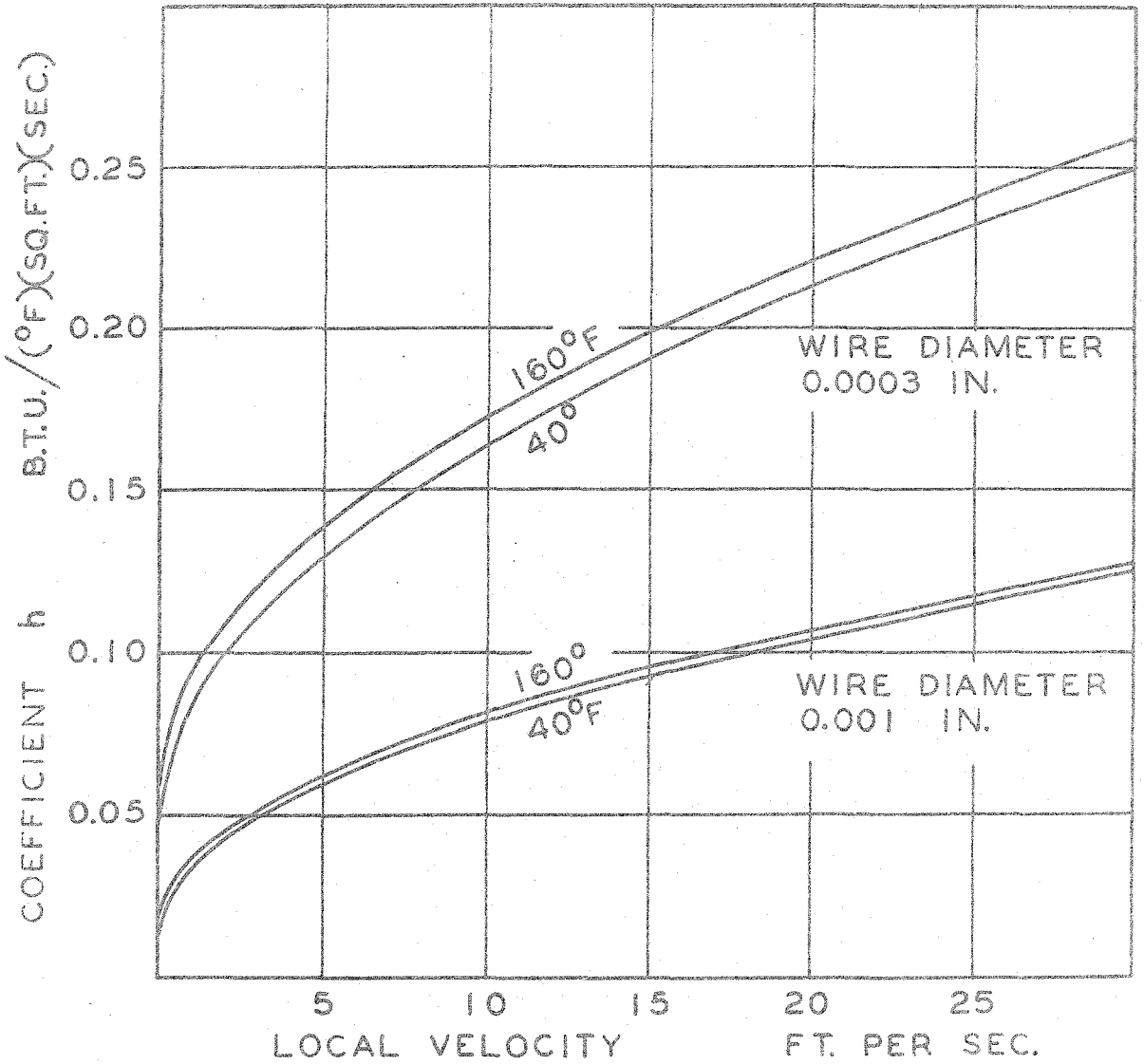


Fig. 5 Convective Thermal Transport Coefficient for Small Wires in Air

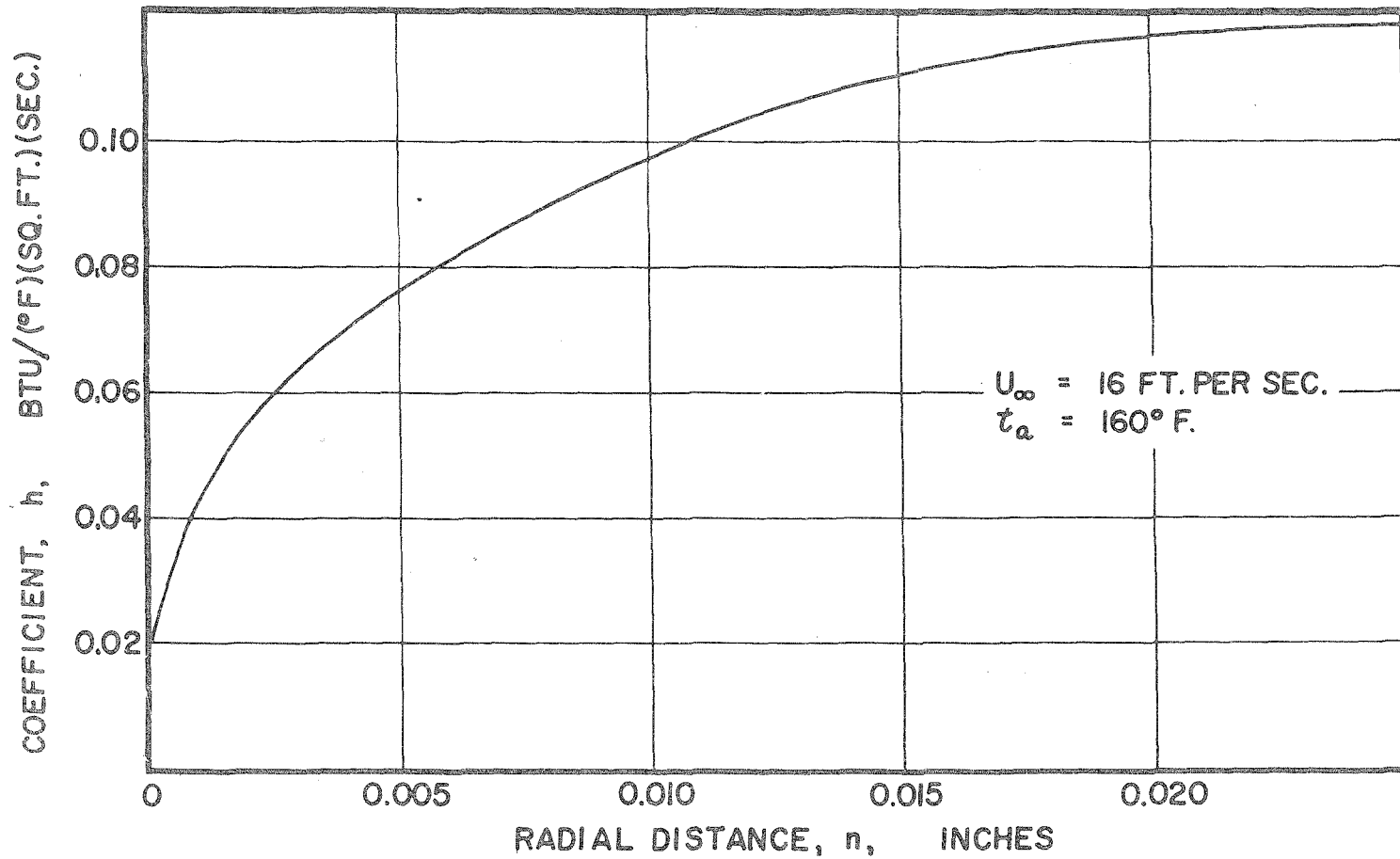


Fig. 6 Convective Heat Transfer Coefficients for 0.001-Inch Diameter Wire near a 0.5-Inch Sphere (17, 18)

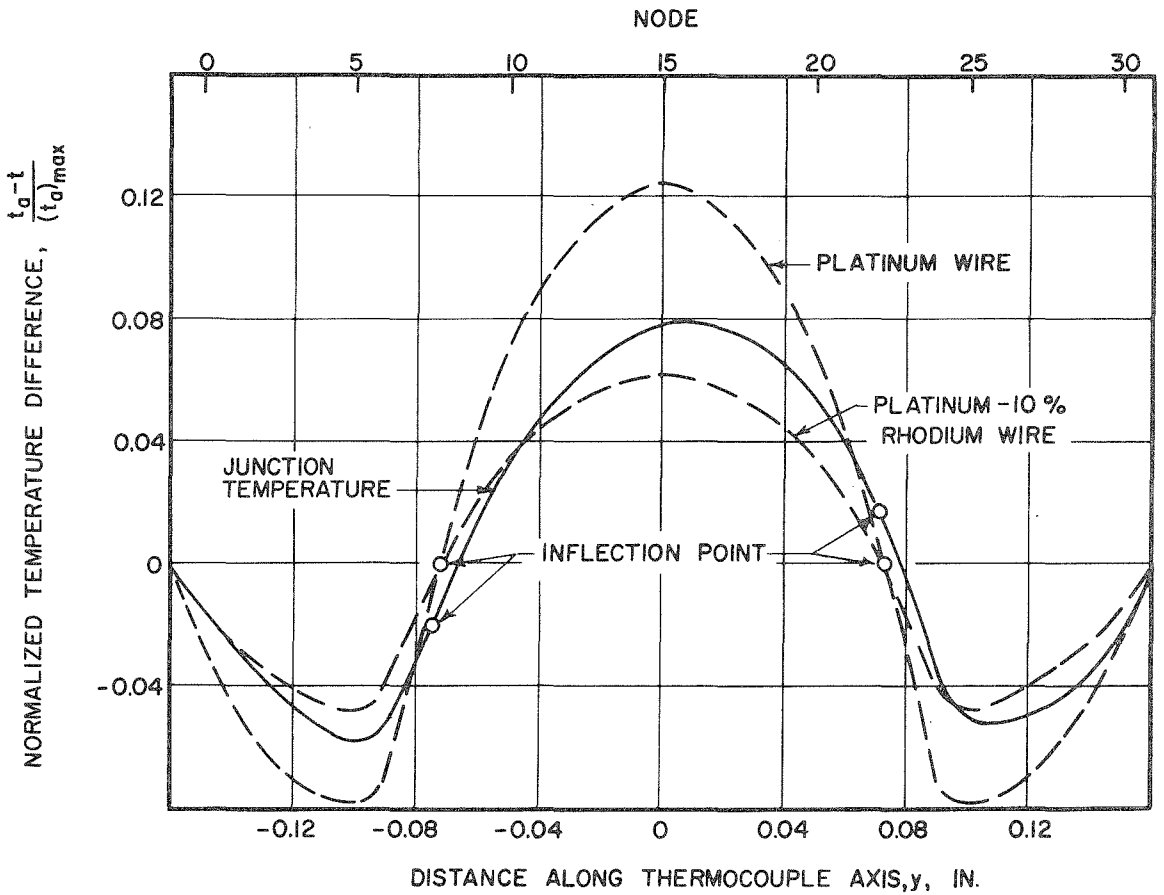


Fig. 7 Normalized Temperature Difference between Wire and Air

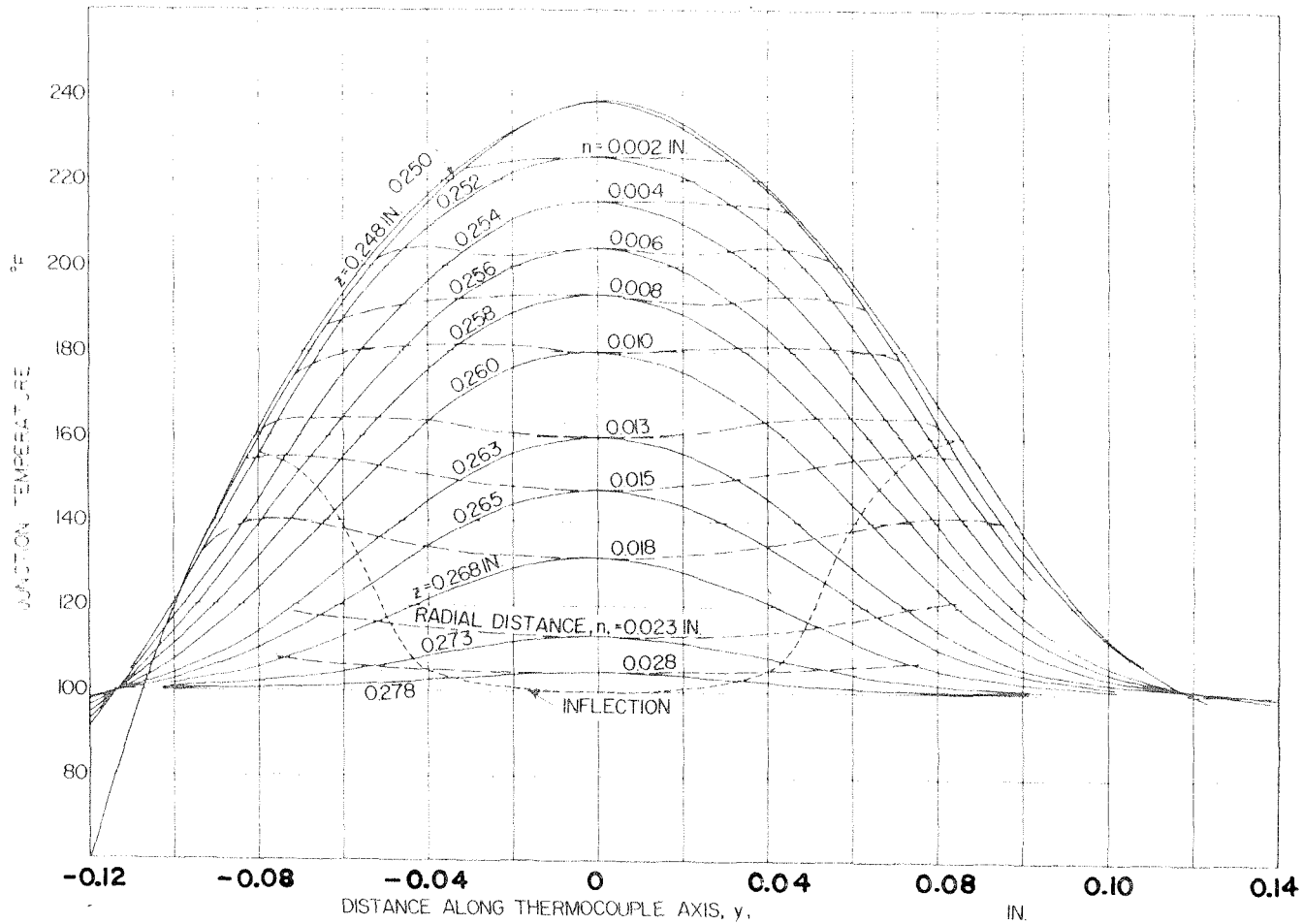


Fig. 8 Experimental Junction Temperatures in Plane of Equator

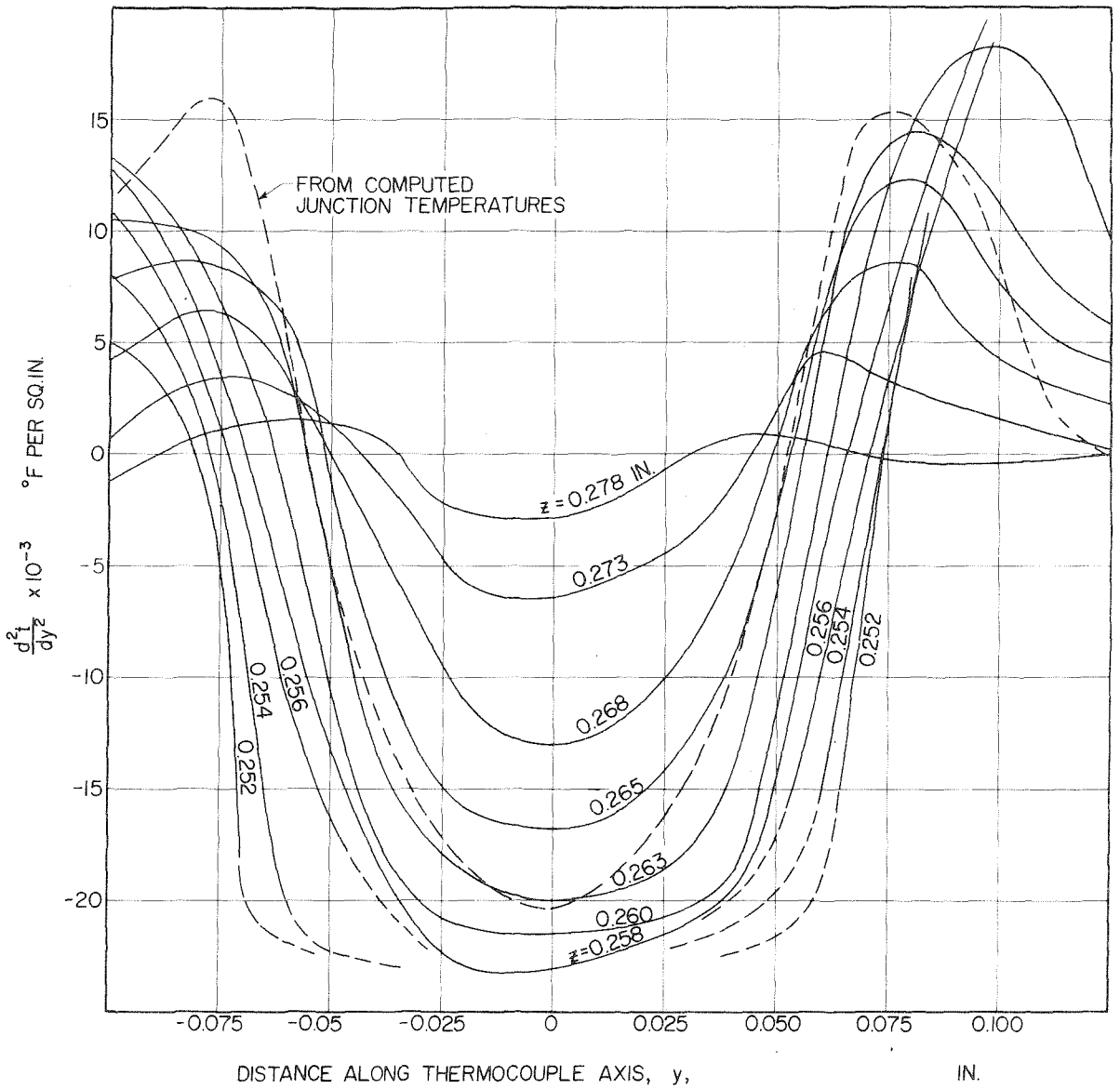


Fig. 9 Second Derivative of Experimental Junction Temperatures

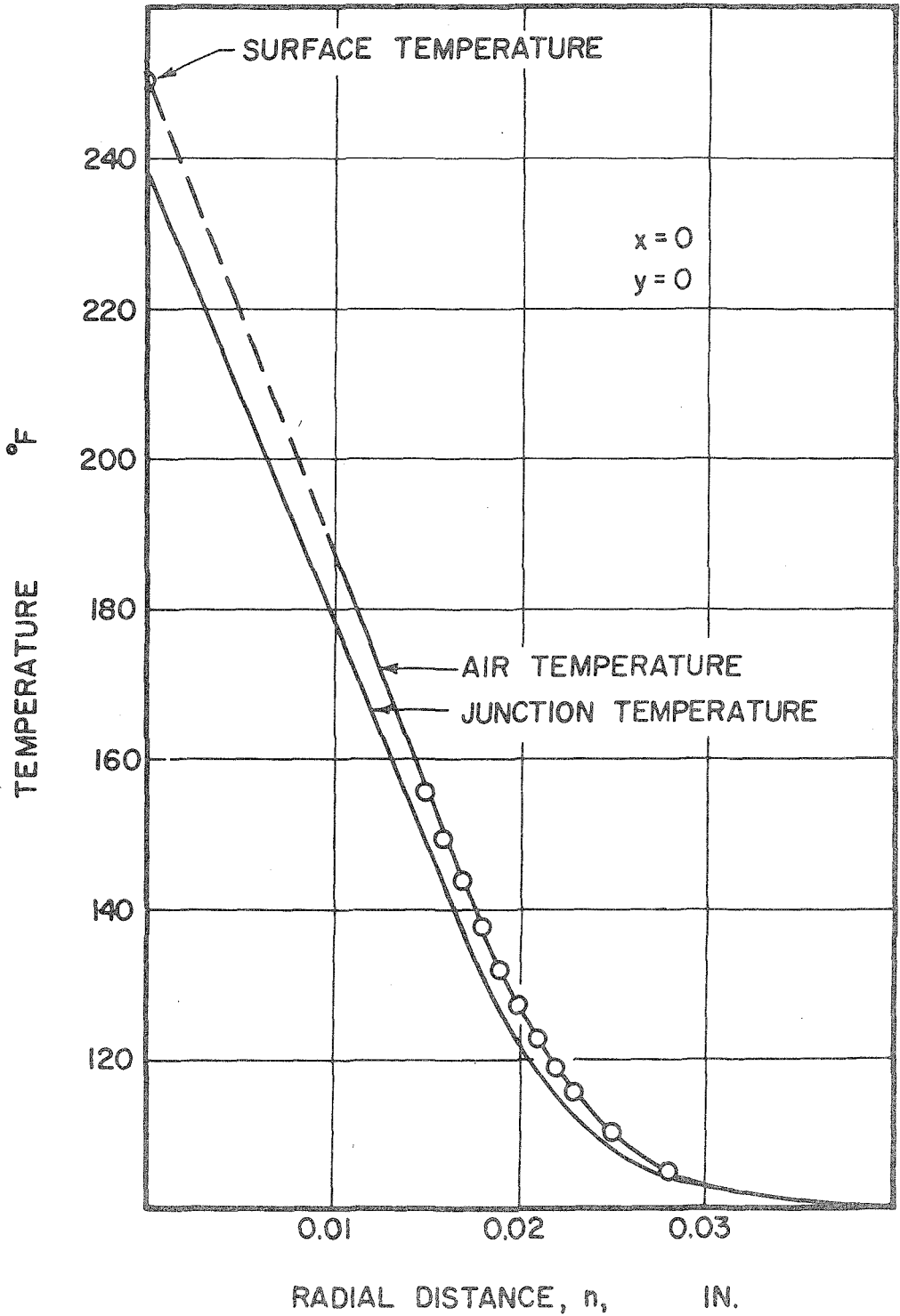


Fig. 10 Radial Temperature Distribution at Equator

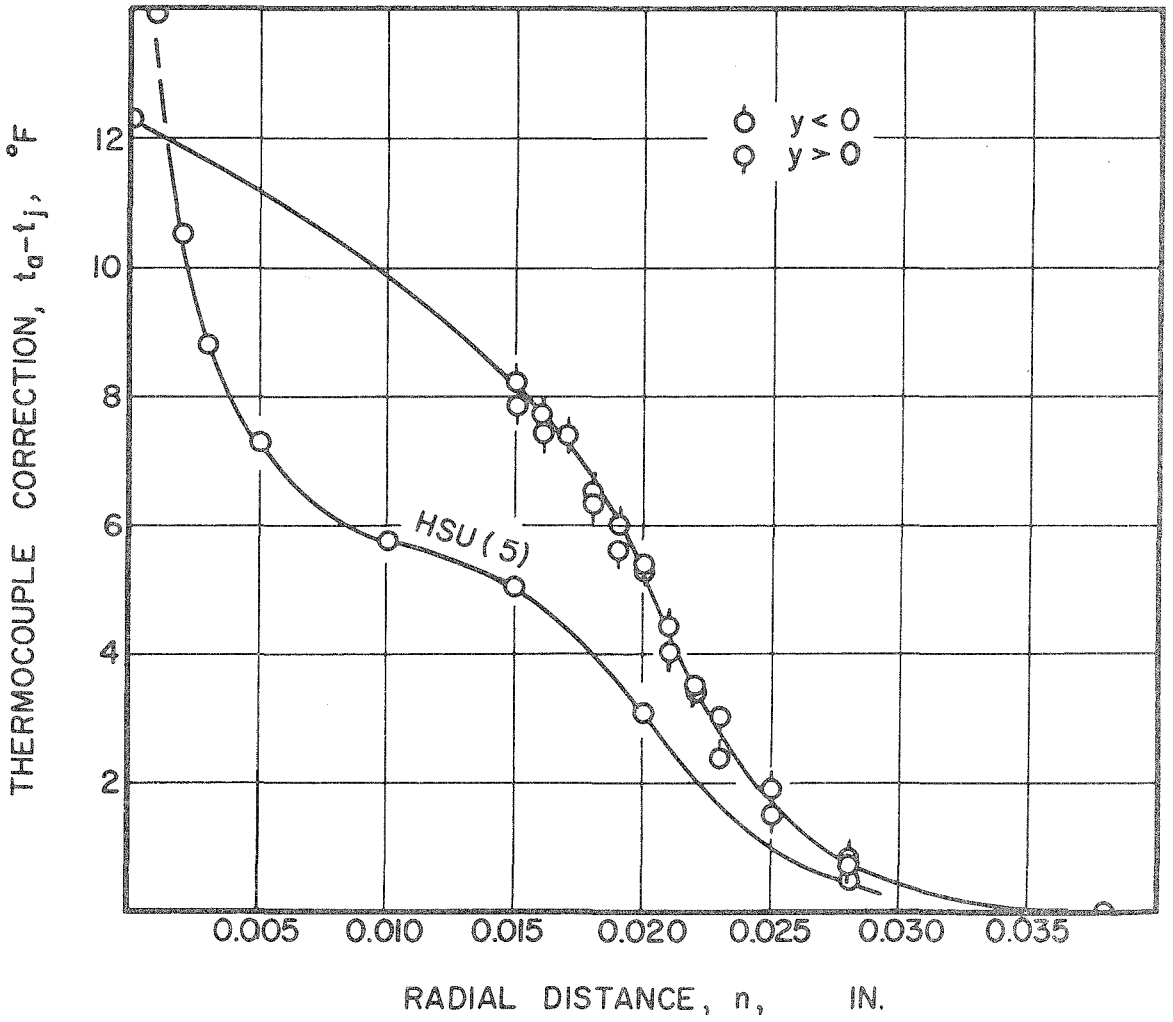


Fig. 11 Conduction Corrections for a 0.001-Inch Diameter Thermocouple

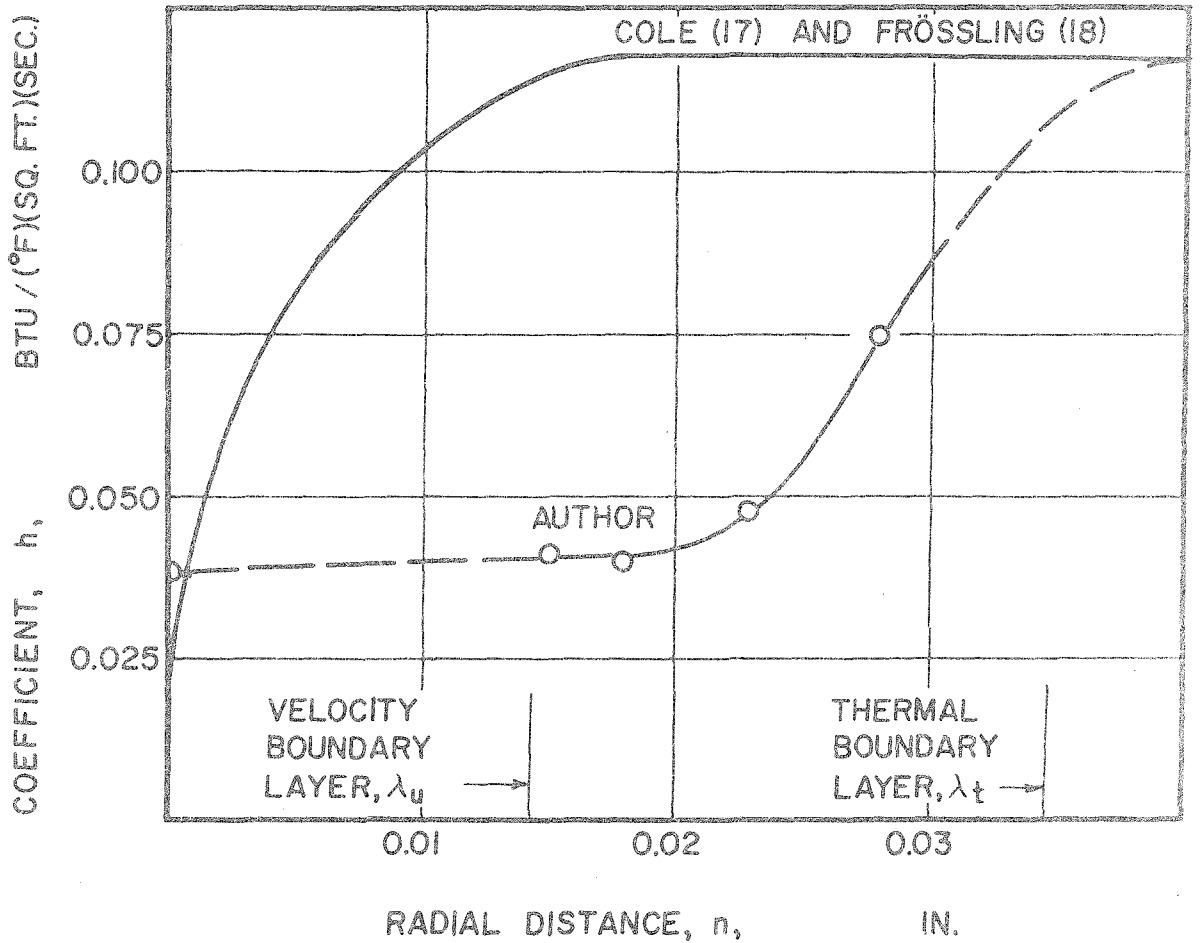


Fig. 12 Experimental Convective Heat Transfer Coefficients for 0.001-Inch Diameter Wire near a 0.5-Inch Sphere

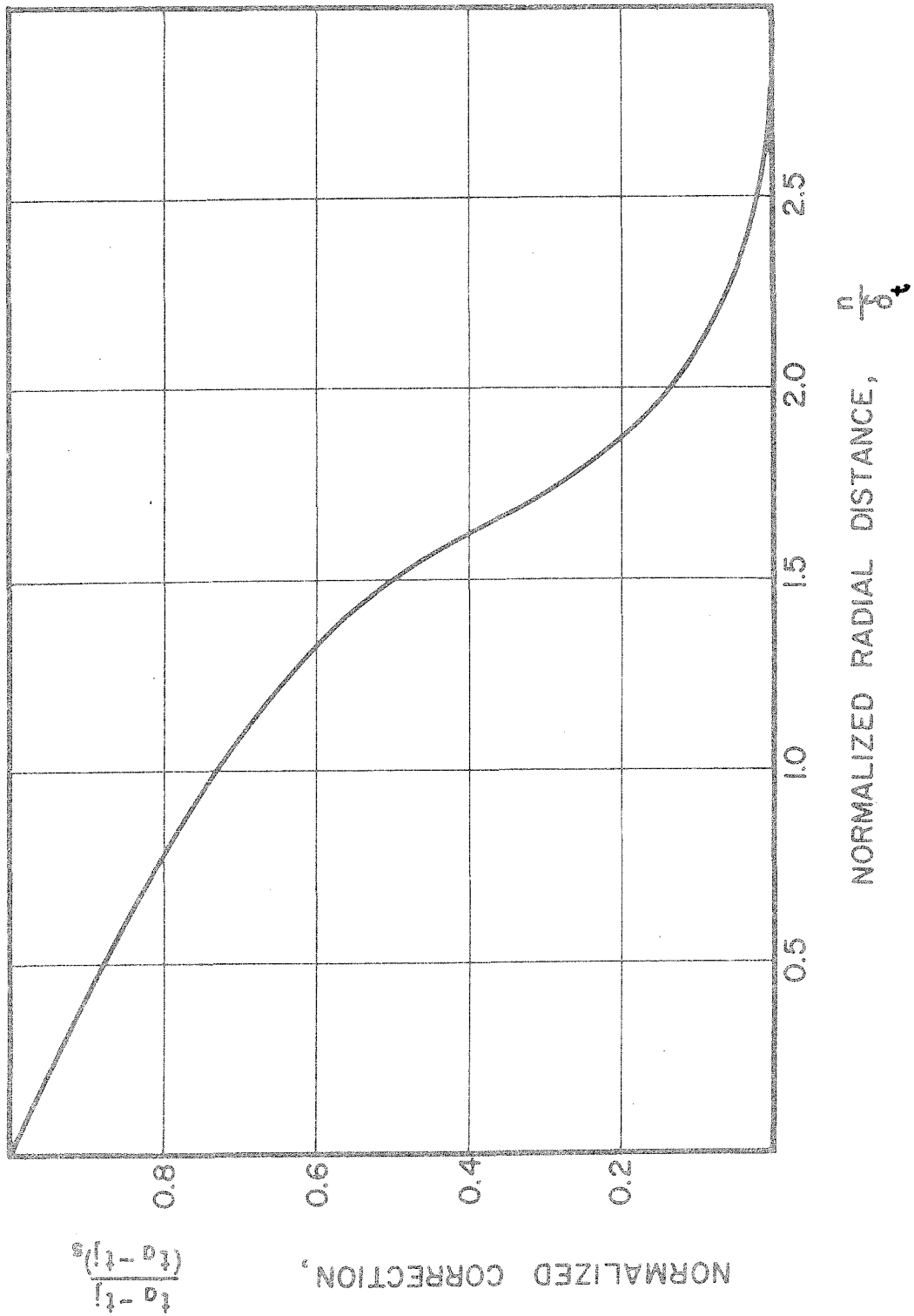


Fig. 13 Dimensionless Conduction Corrections for a 0.001-Inch Diameter Thermocouple

LIST OF TABLES

- I. Computed Wire Temperatures
- II. Experimental Junction Temperatures in Plane of the Equator
- III. Second Derivative with Respect to y of Smoothed Experimental Temperatures
- IV. Heat Transfer Coefficients and Corrections for 0.001-Inch Thermocouple

TABLE I. COMPUTED WIRE TEMPERATURES^a

y in.	Node n	Platinum Wire		Platinum, 10% Rhodium Wire	
		$t_a - t$	d^2t/dy^2 in. ⁻²	$t_a - t$	d^2t/dy^2 in. ⁻²
	-1	0	-	0	-
-0.15	0	-2.45 x 10 ⁻²	35.8	-1.42 x 10 ⁻²	48.1
	1	-4.54	66.3	-2.60	88.2
	2	-6.01	87.8	-3.38	114.7
	3	-6.91	100.8	-3.86	130.9
	4	-7.61	111.0	-4.44	150.6
-0.10	5	-7.70	112.3	-4.80	162.9
	6	-6.01	87.7	-3.90	132.2
	7	-2.48	36.2	-1.60	54.2
	8	0.88	-12.9	0.35	-12.0
	9	3.99	-58.2	2.04	-69.4
-0.05	10	6.87	-100.2	3.62	-122.7
	11	8.88	-129.6	4.55	-154.3
	12	10.18	-148.7	5.03	-170.5
	13	11.24	-164.1	5.47	-185.5
	14	12.19	-178.0	6.03	-204.4
0	15	12.49	-182.4	6.19	-209.8
	16	12.19	-178.0	6.03	-204.4
	17	11.24	-164.1	5.47	-185.5
	18	10.18	-148.7	5.03	-170.5
	19	8.88	-129.6	4.55	-154.3
0.05	20	6.87	-100.2	3.62	-122.7
	21	3.99	-58.2	2.04	-69.4
	22	0.88	-12.9	0.35	-12.0
	23	-2.48	36.2	-1.60	54.2
	24	-6.01	87.7	-3.90	132.2
0.10	25	-7.70	112.3	-4.80	162.9
	26	-7.61	111.0	-4.44	150.6
	27	-6.91	100.8	-3.86	130.9
	28	-6.01	87.8	-3.38	114.7
	29	-4.54	66.3	-2.60	88.2
0.15	30	-2.45	35.8	-1.42	48.1
	31	0	-	0	-

^a All temperatures are normalized with respect to air temperature at y = 0.

TABLE I. (Cont.)

Node n	Air Temperature t_a	Thermocouple Junction at Node 15		Thermocouple Correction	
		$t_a - t$	d^2t/dy^2 in. ⁻²	$t_a - t_j$	d^2t_j/dy^2 in. ⁻²
-1	0	0	-	0	-
0	0	-2.46×10^{-2}	35.9	-1.42×10^{-2}	57.9
1	0.0072	-4.56	66.5	-2.70	100.3
2	0.0272	-6.04	88.2	-3.70	119.5
3	0.0617	-6.96	101.5	-4.45	130.0
4	0.1083	-7.68	112.0	-5.29	150.4
5	0.1721	-7.80	113.8	-5.91	159.8
6	0.2649	-6.16	89.9	-5.23	114.5
7	0.3849	-2.70	39.4	-2.98	25.0
8	0.5068	0.56	-8.1	-0.78	-27.9
9	0.6249	3.52	-51.3	1.31	-77.1
10	0.7349	6.18	-90.2	3.36	-126.6
11	0.8262	7.87	-114.8	4.82	-149.2
12	0.8975	8.71	-127.1	5.76	-161.5
13	0.9514	9.09	-132.6	6.58	-178.9
14	0.9879	9.05	-132.0	7.45	-201.2
15	1.0000	7.89	-267.5	7.89	-202.9
16	0.9879	6.98	-236.8	7.94	-195.7
17	0.9514	6.01	-203.8	7.51	-174.8
18	0.8975	5.33	-180.8	7.08	-164.6
19	0.8262	4.72	-160.1	6.57	-149.9
20	0.7349	3.72	-126.0	5.55	-114.1
21	0.6249	2.10	-71.2	3.80	-55.7
22	0.5068	0.38	-13.0	1.80	-1.3
23	0.3849	-1.58	53.6	-0.56	64.7
24	0.2649	-3.89	131.9	-3.39	143.6
25	0.1721	-4.80	162.7	-4.92	153.7
26	0.1083	-4.44	150.5	-5.10	128.3
27	0.0617	-3.86	130.9	-4.84	111.5
28	0.0272	-3.38	114.6	-4.49	97.8
29	0.0072	-2.60	88.1	-3.66	61.0
30	0	-1.42	48.1	-2.16	5.1
31	0	0	-	0	-

TABLE II. EXPERIMENTAL JUNCTION TEMPERATURES IN PLANE OF THE EQUATOR

y in.	z in.					
	0.248	0.250	0.252	0.254	0.256	0.258
	Temperature °F. minus 100°					
-0.120	-40.13	-	-	-8.39	-6.94	-5.49
-0.100	19.88	20.61	20.72	17.07	13.69	10.86
-0.080	61.48	59.64	55.39	44.93	39.23	31.28
-0.060	93.85	91.34	87.31	75.05	64.38	55.12
-0.040	116.64	115.21	108.67	96.10	86.04	75.57
-0.020	131.56	130.85	121.67	110.86	99.58	88.82
0	138.96	138.27	125.45	115.21	104.02	93.35
0.020	133.41	132.25	120.95	109.85	98.59	88.57
0.040	118.57	117.85	108.43	97.60	85.54	76.09
0.060	96.35	94.60	85.79	75.05	64.64	55.39
0.080	68.04	63.59	57.52	48.43	39.23	32.65
0.100	37.86	33.48	29.62	23.23	17.91	14.25
0.120	12.84	12.28	-	-	6.01	4.87
0.140	-	-0.29	-	-	0.58	0.86

TABLE II. (Cont.)

y in.	z in.					
	0.260	0.263	0.265	0.268	0.273	0.278
	Temperature °F. minus 100°					
-0.120	-3.75	-2.31	-1.73	-	-	-
-0.100	7.44	4.02	2.58	1.43	0.72	0.58
-0.080	24.07	13.97	10.00	5.44	2.01	0.86
-0.060	44.12	29.34	20.72	12.84	4.59	1.43
-0.040	63.59	44.66	34.02	21.56	8.29	2.58
-0.020	76.09	56.18	43.85	28.79	11.70	4.02
0	79.69	59.90	47.36	31.55	12.84	4.45
0.020	75.31	56.18	43.58	27.96	11.42	3.73
0.040	63.33	45.47	34.30	21.00	8.01	2.44
0.060	44.39	29.34	21.56	11.99	4.02	1.43
0.080	24.35	14.82	10.29	5.44	1.86	0.58
0.100	10.29	5.73	4.30	2.30	0.86	0.58
0.120	3.45	2.30	1.43	0.86	-	-
0.140	0.29	0.58	-	-	-	-
0.160	-1.44	-0.86	-	-	-	-

TABLE III. SECOND DERIVATIVE WITH RESPECT TO y OF SMOOTHED EXPERIMENTAL TEMPERATURES

y in.	z in.				
	0.250	0.252	0.254	0.256	0.258
	d^2t/dy^2 °F per in. ² $\times 10^{-3}$				
-0.100	2.38	4.95	7.95	10.8	12.8
-0.080	-3.25	-0.775	1.40	3.55	5.88
-0.060	-33.4	-26.7	-20.0	-13.4	-6.68
-0.040	-22.4	-21.2	-20.0	-18.9	-17.7
-0.020	-16.9	-18.5	-20.1	-21.7	-23.4
0	-30.1	-28.2	-26.3	-24.4	-22.5
0.020	-20.9	-20.6	-20.3	-19.9	-19.6
0.040	-20.4	-20.2	-20.0	-19.8	-19.6
0.060	-26.3	-20.9	-15.5	-10.1	-4.70
0.080	9.23	7.95	7.13	7.10	9.93
0.100	16.3	20.7	24.4	26.6	23.9
0.120	28.0	23.3	18.7	14.6	11.9

TABLE III. (Cont.)

y in.	z in.					
	0.260	0.263	0.265	0.268	0.273	0.278
	d^2t/dy^2 °F per in. ² $\times 10^{-3}$					
-0.100	13.2	10.5	7.75	4.20	0.675	-1.25
-0.080	8.88	9.80	8.63	8.48	3.23	0.725
-0.060	-2.10	4.03	6.05	3.30	2.80	1.45
-0.040	-17.1	-13.2	-8.48	-3.73	-0.725	0.725
-0.020	-21.5	-17.9	-15.8	-11.2	-5.68	-2.53
0	-21.5	-20.1	-18.2	-15.9	-6.40	-2.88
0.020	-17.6	-15.0	-14.5	-8.43	-4.98	-1.43
0.040	-19.1	-14.6	-9.15	-5.13	-1.45	0.700
0.060	-1.40	4.50	6.30	6.15	4.58	0.400
0.080	14.6	14.5	12.3	8.53	2.90	2.13
0.100	18.3	11.2	7.58	4.25	1.60	0.450
0.120	9.45	5.78	4.10	2.20	0.150	0.050

TABLE IV. HEAT TRANSFER COEFFICIENTS AND CORRECTIONS FOR 0.001-INCH THERMOCOUPLE

Radial Distance in.	Normalized Distance $\frac{n^a}{\delta_t}$	Air Temperature			Thermocouple Correction		Normalized Correction Average	$-d^2t/dy^2$ $\frac{y=0}{\text{OF/in.}^2}$	Heat Transfer Coefficient $\frac{\text{Btu}}{(\text{OF})(\text{ft}^2)(\text{sec})}$
		Junction Temperature $y=0$ OF	$y<0$ OF	$y>0$ OF	$y<0$ OF	$y>0$ OF			
0	0	238.27	-	1 -	12.28 ^b		1.00	24×10^3	3.8×10^{-2}
0.015 ^c	1.20	147.36	155.2	155.6	7.8	8.2	0.65	16.8×10^3	4.09×10^{-2}
0.016	1.28	142.20 ^d	149.6	149.9	7.4	7.7	0.62	-	-
0.017	1.36	136.60 ^d	144.0	144.1	7.4	7.5	0.61	-	-
0.018	1.44	131.55	137.9	138.1	6.3	6.5	0.52	13.0×10^3	3.94×10^{-2}
0.019	1.52	126.30 ^d	131.9	132.3	5.6	6.0	0.47	-	-
0.020	1.60	122.05	127.5	127.4	5.4	5.3	0.44	-	-
0.021	1.68	118.45 ^d	122.4	122.8	4.0	4.4	0.34	-	-
0.022	1.75	115.45 ^d	118.9	118.8	3.5	3.4	0.28	-	-
0.023	1.84	112.84	115.8	115.2	3.0	2.4	0.22	6.40×10^3	4.69×10^{-2}
0.025	2.00	108.60 ^d	110.5	110.1	1.9	1.5	0.14	-	-
0.028	2.24	104.45	105.1	105.2	0.7	0.8	0.06	2.88×10^3	7.44×10^{-2}
0.038	3.04	100.58	-	-	0	0	0	-	-

^a Thermal boundary layer thickness, δ_t , was 0.0125 in.

^b Obtained from surface temperature of sphere, which was 250.55°F.

^c No inflection points in region $0 < n < 0.015$.

^d Values obtained from Figure 9.

Part II

LOCAL CONVECTIVE HEAT TRANSFER FROM A SPHERE*

* The material presented in Part II will be submitted to the American Society of Mechanical Engineers for publication under the joint authorship of W. W. Short and B. H. Sage.

INTRODUCTION

The macroscopic heat transfer from spheres to fluids has been investigated for a large range of flow conditions and sphere sizes. McAdams (1) summarized much of the available data obtained for moderate flow conditions. Recent studies of macroscopic heat transfer were concerned with extreme conditions of pressure, velocity and turbulence for which the heat transfer as expressed by the Nusselt number can not be correlated as a single-valued function of Reynolds number. There was much interest in supersonic flow in which compressible effects are important. Beckwith (2) measured the heat transfer from a 3.5-inch sphere at Mach numbers of 2.00 and 4.15. Tests made by Eberly (3) showed that energy accommodation and viscous slip at the surface of a sphere are important factors governing heat transfer at low pressures. Sato (4) demonstrated that a turbulence level of 0.15 increased the macroscopic heat transfer at a Reynolds number of 8000, by 40 per cent over that for laminar flow at the same Reynolds number.

There is little information pertaining to local heat transfer from spheres even at moderate conditions. The effect of extreme conditions on the macroscopic heat transfer might be predicted if the mechanism of local heat transfer is thoroughly understood. Some data on local heat and material transfer were obtained by measuring the rate of solution or sublimation of solid spheres (5,6,7). Recent investigators have employed equipment for the direct measurement of the local heat transfer. Cary (8) and Xenakis (9) measured the energy loss from a small heated

plug set in the surface of a sphere, but insulated from the sphere. Cary (8) determined the local transfer from a five-inch iron sphere to an air stream at Reynolds numbers up to 1.5×10^5 . Xenakis and co-workers (9) repeated some earlier measurements by Lautman and Droege (10) with spheres 6, 9, and 12 inches in diameter. Hsu (11) established the local heat transfer from air-temperature gradients measured in the boundary layer surrounding 0.5-inch spheres. Hsu presented, as a function of polar angle, data on heat transfer alone and data on simultaneous heat and material transfer at Reynolds numbers between 1500 and 4200 at 0.054 level of turbulence.

The accuracy of theoretical solutions for the temperature distribution in the boundary layer of a sphere is limited by the assumptions employed in solving for velocities in the momentum boundary layer. The flow near the forward stagnation point is better understood than at any other point on a sphere. Frössling (12), Sibulkin (13), and Korobkin (14) computed Nusselt numbers for the stagnation point. Drake (15) and Sibulkin (16) derived equations for the heat transfer as a function of position in the upstream hemisphere. No theoretical analysis of heat transfer in the downstream hemisphere, where separation of the boundary layer occurs, was found. Heat transfer in the highly turbulent wake can not be treated by the methods used in the solutions cited above, all of which assume laminar flow in the boundary layer.

In the present study, temperature measurements were made in the boundary flows surrounding a 0.5-inch sphere at Reynolds numbers between

800 and 7100. Sufficient data were obtained to establish the temperature distribution in the boundary layer up to the separation point. These measurements were carried out in an air stream at a turbulence level of 0.013. The local thermal transport was established from the radial temperature gradients adjacent to the sphere.

ANALYSIS

The Reynolds numbers presented in this investigation are based upon the properties of the free stream as indicated in the following equation:

$$Re_{\infty} = \frac{D U_{\infty}}{\nu_{\infty}} \quad (1)$$

The macroscopic Nusselt number based on the thermal conductivity of air at the surface of the sphere is evaluated from the following expression:

$$Nu_i^* = \frac{\bar{Q} D}{(t_i^* - t_{\infty}) k_i^* A} \quad (2)$$

In addition, the macroscopic Nusselt number based on the free stream properties is determined from:

$$Nu_{\infty}^* = \frac{\bar{Q} D}{(t_i^* - t_{\infty}) k_{\infty} A} \quad (3)$$

The space-average surface temperature, t_i^* , required in Equations 2 and 3 is defined by the following equation:

$$t_i^* = \frac{1}{A} \int_0^A t_i dA \quad (4)$$

The local Nusselt number, based on the molecular characteristics of the fluid at the surface, is defined by:

$$Nu_i = \frac{\dot{Q} D}{(t_i - t_{\infty}) k_i} \quad (5)$$

The local thermal flux, \dot{Q} , is established from:

$$\dot{Q} = -k_i \left(\frac{\partial t}{\partial n} \right)_i \quad (6)$$

where n is the distance normal to the surface of the sphere. The local thermal flux is integrated with respect to the surface area of the sphere to obtain the total thermal flux from the sphere.

$$\underline{\dot{Q}} = \int_0^A \dot{Q} dA \quad (7)$$

A relative Nusselt number is found to be more useful in this instance than the local Nusselt number defined by Equation 5. The relative Nusselt number is the ratio of the local Nusselt number to the macroscopic Nusselt number as shown in the following equation:

$$\frac{Nu_i}{Nu_i^*} = \frac{(t_i^* - t_\infty) k_i A \bar{Q}}{(t_i - t_\infty) k_i \int_0^A \dot{Q} dA} \quad (8)$$

The relative Nusselt number can be used to advantage to portray the distribution of local transport for several velocities.

It is convenient to consider a thermal boundary layer whose thickness is defined as:

$$\delta_t = \int_0^\infty \Upsilon dn \quad (9)$$

The term Υ is the normalized temperature defined by the following relation:

$$\Upsilon = \frac{t - t_\infty}{t_i - t_\infty} \quad (10)$$

It has been found (11) that the normalized temperature may be approximated by an empirical expression in which the function ϕ is that developed by Blasius (17).

$$\Upsilon = 1 - \phi\left(\frac{n}{\delta_t}\right) \quad (11)$$

It should be emphasized that Equation 11 predicts only approximately the temperature in the boundary layer and is not suitable for computing

temperature gradients and local heat transfer rates.

METHODS AND EQUIPMENT

In this investigation temperature distributions were determined about a silver sphere 0.5 inch in diameter. The sphere was suspended in an air stream having a temperature of 100°F, and measurements were carried out at gross stream velocities of 4, 8, 16, and 32 feet per second.

The level of turbulence was established by the method described by Schubauer (18). The transverse turbulence level was found to be 0.013 from the divergence of the temperature wake of a small heated wire. The transverse level of turbulence is defined as the ratio of the root-mean-square of the transverse component of the fluctuating velocity to the average velocity. Hsu (11) carried out an investigation with the equipment used in the present study under conditions of artificially induced turbulence.

The silver sphere used in these investigations was described in detail by Baer (19). It consisted of an interior copper sphere upon which a spiral groove was cut, and a chromel heater with glass insulation was placed in the groove. The heater was covered by two silver, hemispherical shells soldered to the surface of the copper sphere. Four copper-constantan thermocouples were placed in a groove cut in the inner surface of the silver shell. These thermocouples indicated the external surface temperature to within 0.01°F. The device was supported by two stainless steel tubes in which the leads to the heater and thermocouples were located. Two small heaters were wound on the supporting tube to

reduce energy loss from the sphere by conduction along the supports. The current to these heaters was adjusted until the internal thermocouples indicated equal temperatures when on the equator normal to the air stream. The energy input to the sphere heater was measured by a circuit of calorimeter type. The total thermal flux from the sphere, as measured by the calorimeter circuit, is believed known to within 0.2 per cent.

The equipment furnishing the air stream was described by Hsu (20). The gross velocity of the air stream was determined from its temperature and weight rate of flow measured by means of a venturi meter (21). The temperature of the air stream was measured to within 0.1°F by means of a platinum resistance thermometer of the coiled-filament type (22). The gross air velocity at the test section was known to within 4 per cent and the temperature did not vary more than 0.2°F (23). The humidity was measured with an uncertainty of less than 0.0001 weight fraction water and the pressure was known within 0.02 per cent.

The local temperature of the air surrounding the sphere was measured with a platinum, constantan thermocouple 0.001 inch in diameter. The thermocouple was soldered to the needles of a probe (11). The reference junction was placed on the probe in the free stream at a distance of approximately one inch from the sphere. Such an arrangement reduced the effect upon the differential measurements of fluctuations in the temperature of the free stream with time. The thermocouple probe was mounted on a traversing mechanism to determine the position of the thermocouple within ± 0.0005 inch relative to three coordinate axes at the center of

the sphere. A series of horizontal and vertical traverses were made with the probe for each condition of flow. The platinum, constantan thermocouple was calibrated under static conditions. A White potentiometer was employed for the measurement of the electromotive force. It is believed that the temperature of the junction was determined within 0.1°F relative to the temperature of the air stream.

EXPERIMENTAL RESULTS

The experimental conditions observed during the eight tests in this investigation are recorded in Tables I and II. In these tables the conditions of flow, Reynolds number, macroscopic Nusselt numbers, average surface temperature and total thermal flux are recorded. The dimensionless groups were computed from equations 1, 2, and 3. The macroscopic Nusselt numbers agree with the data obtained by Sato (4), and are about 10 per cent lower than the correlation recommended by McAdams (1). The properties of air employed in this study are based upon the values selected by Page (24). The average surface temperature was computed from data obtained from the four copper-constantan thermocouples using equation 4. The variation of surface temperature with respect to position is shown in Table III. The normalized surface temperature as a function of polar angle and gross velocity were presented by Sato (4). The thermal flux established from the electrical power dissipated in the sphere was multiplied by 1.0188 to obtain the total observed thermal flux. This factor is the ratio of the surface area of a 0.5-inch sphere to that of the laboratory sphere which was supported by two tubes

0.096 inch in diameter.

The temperatures of the probe thermocouple when in contact with the sphere are listed in Table III together with the surface temperature at several polar angles for each test. These temperatures differ from each other by as much as 34°F at some positions. This apparent discontinuity at the surface is believed to be the result of temperature gradients along the wires supporting the thermocouple junction. Similarly other junction temperatures observed in the thermal boundary layer are lower than the temperature of the air surrounding the wire. For this reason measurements obtained with the probe thermocouple will be termed "wire temperatures"* to distinguish them from the true air temperature. A method of predicting air temperatures from wire temperatures is available (25); however, the necessary heat transfer coefficients for wires in a boundary layer have not been determined. The information presented in this paper is based upon wire temperatures. Two typical wire temperature traverses are shown in Table IV. The detailed traverse data covering all eight tests recorded in Tables I and II are available (26).

The radial wire temperature gradients presented in Table III are computed from the slope of the traverse data near the surface of the sphere. The polar angle listed in Table III is the angle at the center of the sphere between the forward stagnation point and the point at which a traverse intersected the sphere. The radial wire temperature gradient may differ measurably from the radial air temperature gradient at a point

- - - - -
* The term "junction temperature" was used in this sense in Part I

on the surface of the sphere. It is for this reason that the relative Nusselt number is employed. However, if the ratio of the air and wire temperature gradients is independent of polar angle for a particular set of conditions, the relative Nusselt number computed from the wire temperature gradient is correct. Relative Nusselt numbers computed from equation 8 are presented in Table III and plotted in Figure 1. The average of the differences between the relative Nusselt numbers obtained at each velocity and polar angle is 0.040. With the exception of the data at 4 feet per second for the stagnation point, the curves in Figure 1 were drawn to within 0.040 of the experimental points. The local Nusselt numbers, Nu_i , are computed from the relative Nusselt numbers, Nu_i / Nu_i^* and the macroscopic Nusselt number, Nu_i , obtained for each test listed in Table II. The local Nusselt numbers smoothed with respect to Reynolds number and polar angle are listed in Table V and plotted in Figure 2.

The thermal boundary layer thicknesses defined by equation 9 were computed from wire temperatures. This did not introduce an appreciable error in the results because the wire temperature at the surface was used in place of the surface temperature, t_s , in equation 10. If the ratio of the wire temperature and air temperature in each traverse is independent of radial distance, the normalized wire and air temperatures are equal. The thermal boundary layer thickness was established for each point at which a temperature traverse intersected the sphere, with one exception. The thermal boundary layer thickness was not computed at polar angles greater than 121° because the extremely large values

which would be obtained in the turbulent wake would have very little significance. The thermal boundary layer thicknesses are presented as a function of polar angle at four Reynolds numbers in Figure 3, and are listed in Table III.

DISCUSSION OF RESULTS

The curves in Figure 1 for velocities of 16 and 32 feet per second indicate maximum heat transfer at polar angles of approximately 30° and 60° , respectively. The data which Beckwith (2) obtained at Mach 2 show more than a two fold increase of heat transfer at polar angle of 40° over that at the stagnation point. This increase was attributed to the transition from laminar flow to turbulent flow in the boundary layer. A similar situation may have occurred in the present tests.

For comparison with the work of other investigators, the ratio of the local Nusselt number to the macroscopic Reynolds number, Nu_i / \sqrt{Re} is plotted in Figure 4. This curve in Figure 4 is an arithmetic average at each polar angle of the values of Nu_i / \sqrt{Re} obtained in the eight tests. The values of Nu_i / \sqrt{Re} were computed by multiplying together the relative local Nusselt number, Nu_i / Nu_i^* , and the value Nu_i^* / \sqrt{Re} determined for each test. The macroscopic values of Nu_i^* / \sqrt{Re} are nearly constant for the tests presented here, having a value of 0.541 ± 0.013 . For this reason a plot of Nu_i / \sqrt{Re} for each Reynolds number investigated would appear identical to the curves in Figure 1. By the single average curve shown in Figure 4 the author is not suggesting that the ratio Nu_i / \sqrt{Re} is solely a function of polar angle. On the

contrary, Figure 1 indicates that Nu_i / \sqrt{Re} is a function of the free stream velocity.

The present data compare well with the theoretical prediction of Drake (15), especially near the stagnation point. The theories proposed by Sibulkin (13,16), Korobkin (14) and Frossling (12) predict higher heat transfer rates than found in the present study. It should be emphasized that the theoretical analyses assume laminar flow in the boundary layer and do not consider the influence of turbulence in the primary air stream. For this reason it is not surprising that disagreements exist between the predicted and experimental values.

It has been demonstrated that the relative local heat transfer tends to decrease in the upstream hemisphere and increase in the downstream hemisphere as the level of turbulence in the air stream increases. The experimental data of Hsu which are plotted in Figure 4 appear to bear this out. The work of Hsu (11) was carried out at 0.054 level of turbulence, whereas the level of turbulence in this study was 0.013. Cary (8) did not report the turbulence in the free air stream. If this relation between Nusselt number and turbulence level can be applied to the 5-inch-diameter sphere employed by Cary, the turbulence in the air stream appears to have been very high. The data of Xenakis (10) obtained from spheres 6, 9, and 12 inches in diameter do not follow this trend.

The theoretical data, which correspond to a zero level of turbulence, follow the experimental trend of decreasing relative heat transfer with increasing turbulence level at a fixed Reynolds number in the upstream hemisphere.

NOMENCLATURE

A	surface area of sphere, sq. ft.
D	diameter of sphere, ft. or inch
k	thermal conductivity of air, Btu/(°F)(ft.)(sec.)
n	radial or normal distance from surface of sphere, ft.
Nu	Nusselt number
\dot{Q}	local thermal flux from surface, Btu/(sq.ft.)(sec.)
\dot{Q}	total thermal flux from surface, Btu/sec.
Re	Reynolds number
t	temperature, °F
U_{∞}	bulk or free stream velocity, ft./sec.
x	distance from center of sphere along axis parallel to air stream, inch
Υ	normalized temperature ratio
δ_t	thermal boundary layer thickness, ft.
ν	kinematic viscosity, sq. ft./sec.
ϕ	Blasius function

Subscripts

i	solid-gas interface
∞	free air stream

Superscripts

*	space average
---	---------------

REFERENCES

1. McAdams, W. H., "Heat Transmission," 3rd ed., McGraw-Hill Book Co., New York, 265, 1954.
2. Beckwith, I. E., and Gallagher, J. J., NACA TN 4125 (1957).
3. Eberly, D. K., Report No. HE 150-140, Univ. of Calif., Berkeley (1957).
4. Sato, K., and Sage, B. H., ASME Paper No. 57-A-20 (1957).
5. Frossling, N., Gerlands Beit., 52, 170-216 (1938).
6. Mathers, W. G., Madden, A. J., and Piret, E. L., Ind. Eng. Chem., 49, 961 (1957).
7. Frisch, H. L., J. Chem. Phys., 22, 123 (1954).
8. Cary, J. R., Trans. ASME, 75, 483 (1953).
9. Xenakis, G., Amerman, A. E., and Michelson, R. W., Tech. Report 53-117, Wright Air Dev. Center, (1953).
10. Lautman, L. G., and Droege, W. C., Serial No. AIRL A6118 50-15-3, Air Material Command (1950).
11. Hsu, N. T., and Sage, B. H., A.I.Ch.E. Journal, 3, 405-410 (1957).
12. Frössling, N., Lunds. Univ. Årsskrift, N. F. Ård 2.36, No. 4 (1940); English translation NACA TM 1432 (1953).
13. Sibulkin, M., J. Aero. Sci., 19, 570 (1952).
14. Korobkin, I., ASME Paper No. 54-F-18 (1954).
15. Drake, R. M., J. Aero. Sci., 20, 309 (1953).
16. Sibulkin, M., unpublished (1952); information in reference 15.
17. Blasius, H., Z. angew Math. u. Phys., 56, 1 (1908).
18. Schubauer, G. B., NACA Report No. 524 (1953).
19. Baer, D. H., Schlinger, W. G., Berry, V. J., and Sage, B. H., J. Appl. Mech., 20, 407 (1953).

20. Hsu, N. T., Reamer, H. H., and Sage, B. H., ADI Publications, Library of Congress, Washington D. C., Doc. No. 4219 (1954).
21. Corcoran, W. H., Page, F., Schlinger, W. G., and Sage, B. H., Ind. Eng. Chem., 44, 410 (1952).
22. Meyers, C. H., Bur. Std. J. Research, 9, 807 (1932).
23. Sato, K., Ph.D. thesis, Calif. Inst. Tech. (1955).
24. Page, F., Corcoran, W. H., Schlinger, W. G., and Sage, B. H., Ind. Eng. Chem., 44, 419 (1952).
25. Short, W. W., Ph. D. thesis Part I, Calif. Inst. of Tech. (1958).
26. Laboratory data to be submitted to the Am. Doc. Inst., Library of Congress, Washington, D. C.
27. Short, W. W., and Sage, B. H., "Effect of Turbulence on Local Heat Transfer," submitted to the J. of Appl. Mech.

LIST OF FIGURES

1. Variation of Relative Local Nusselt Number with Polar Angle
2. Variation of Local Nusselt Number with Polar Angle
3. Variation of Thermal Boundary Layer Thickness with Polar Angle
4. Comparison of Local Transport with Several Investigators

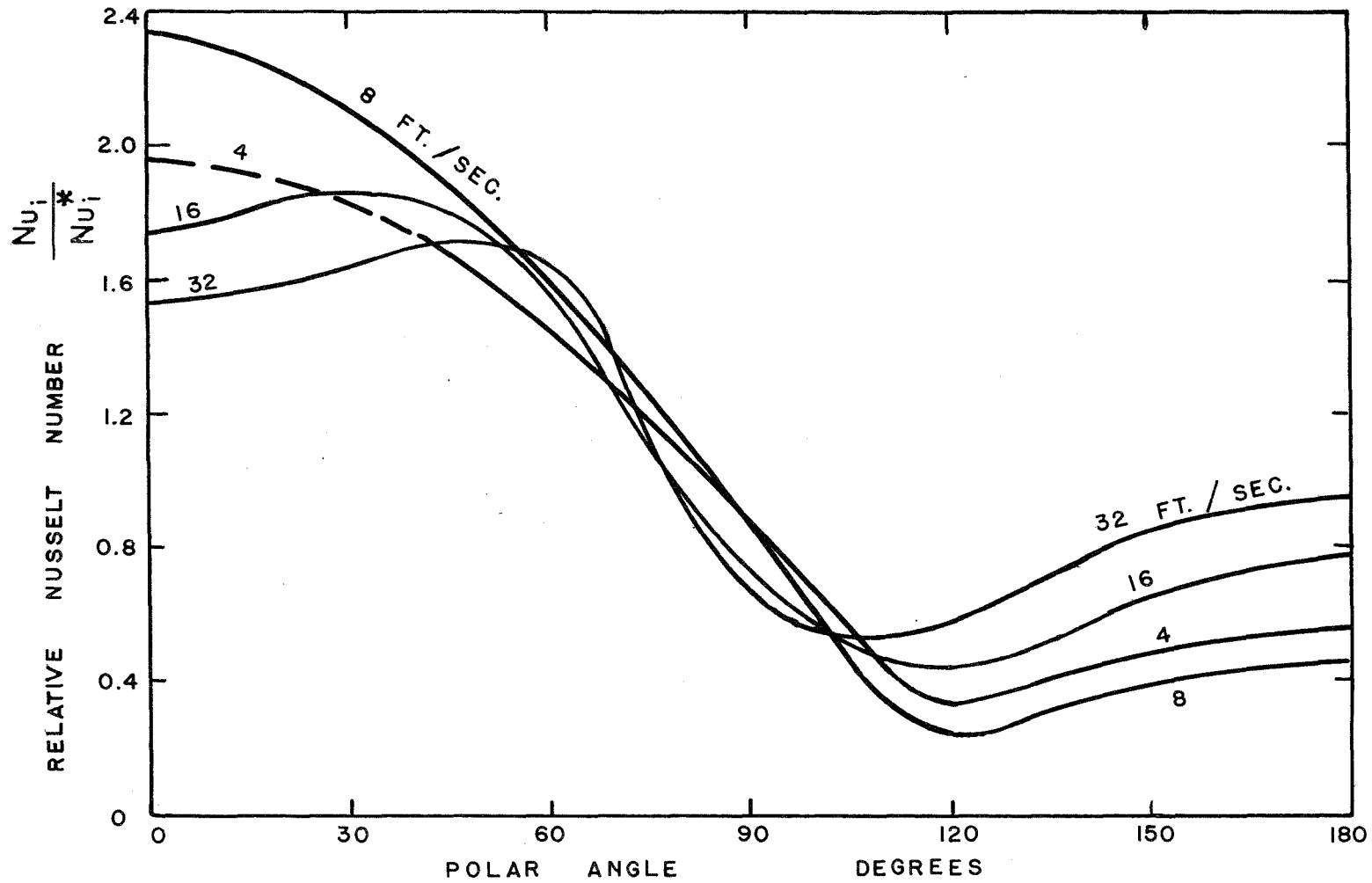


Fig. 1. Variation of Local Nusselt Number with Polar Angle

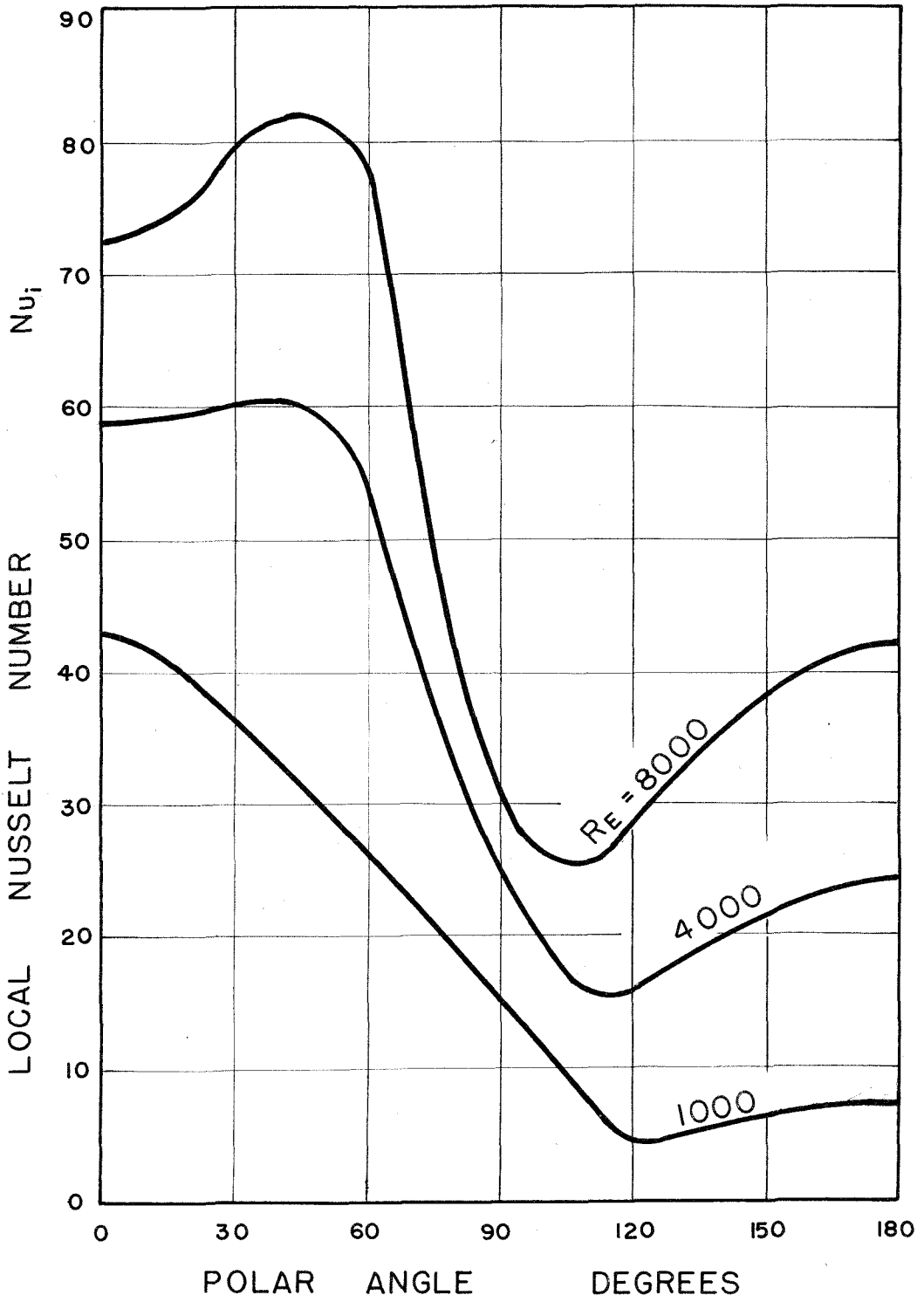


Fig. 2. Variation of Local Nusselt Number with Polar Angle

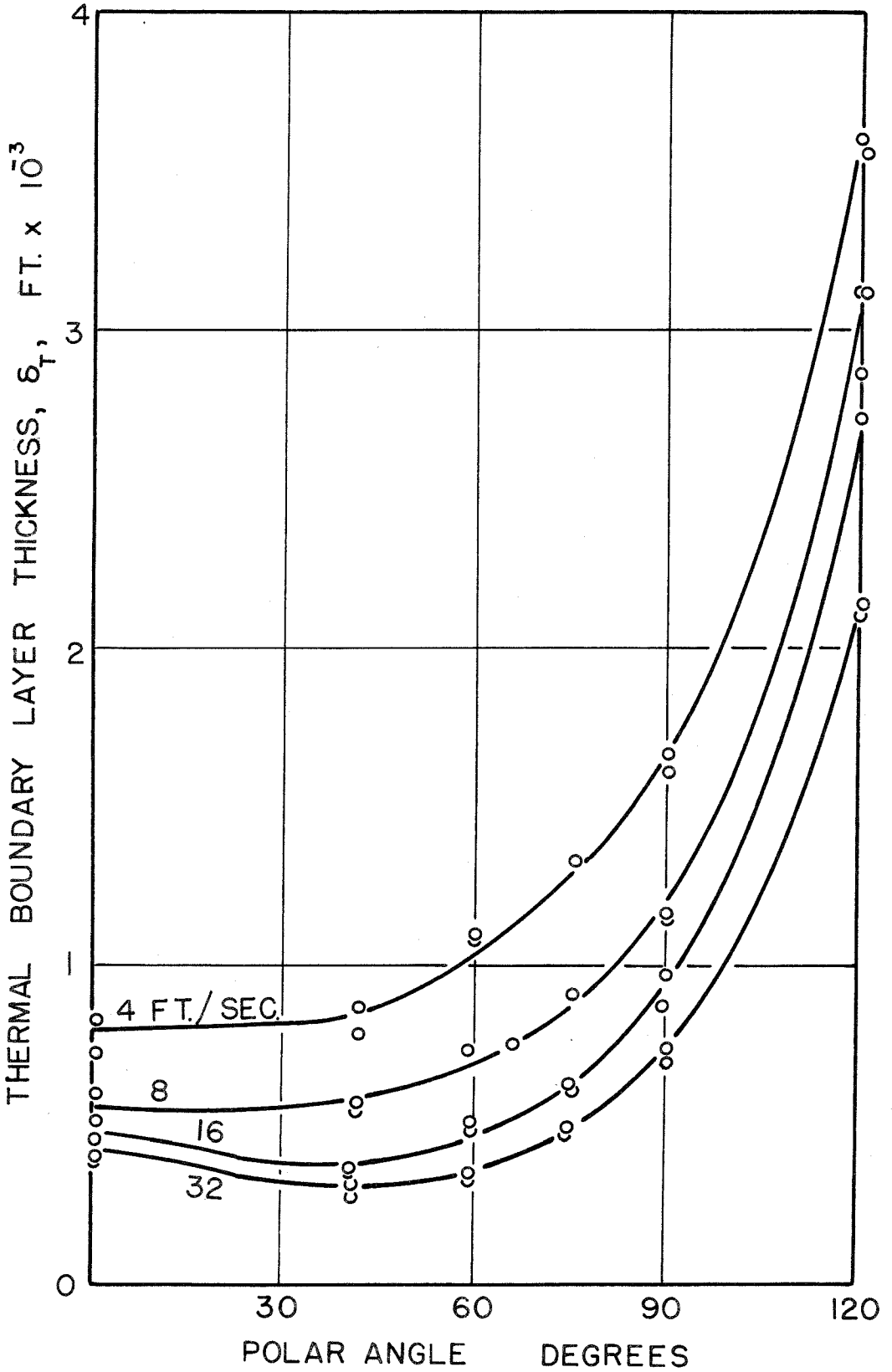


Fig. 3. Variation of Thermal Boundary Layer Thickness with Polar Angle

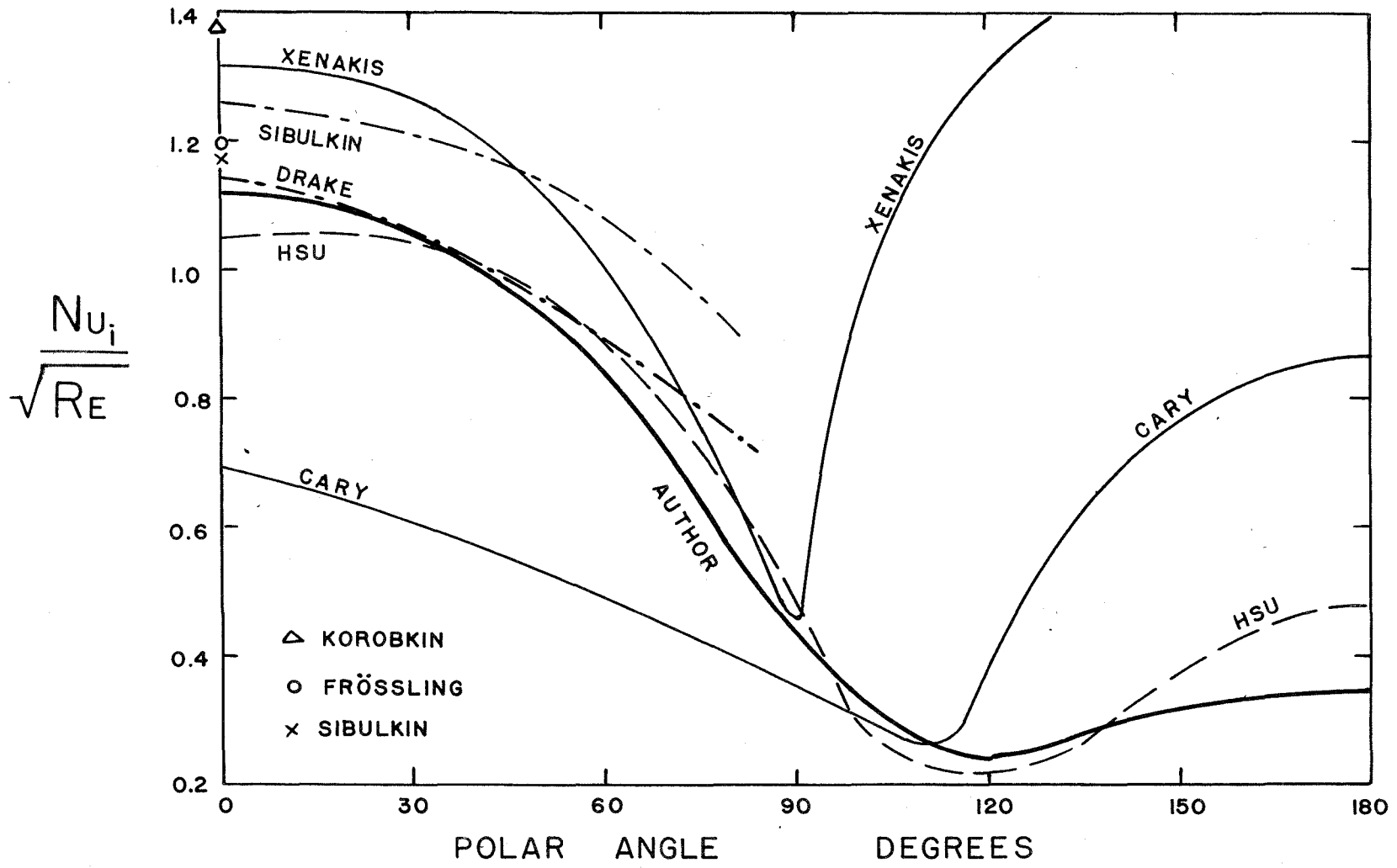


Fig. 4. Comparison of Local Transport with Several Investigators

LIST OF TABLES

- I. Experimental Conditions in Air Stream
- II. Macroscopic Thermal Transport From a 0.5-Inch Heated Sphere
- III. Experimental Conditions in Boundary Layer of a 0.5-Inch Heated Sphere
- IV. Typical Horizontal Temperature Traverse Data From Test 62
- V. Smoothed Local Nusselt Numbers

TABLE I. EXPERIMENTAL CONDITIONS IN AIR STREAM

Test Number	Velocity ft./sec.	Temperature °F.	Pressure lb./sq.ft. Absolute	Weight Fraction Water	Reynolds Number
63	4.06	100.11	2066.3	0.0081	888
65	4.06	100.12	2062.8	0.0072	882
62	8.03	100.15	2067.9	0.0072	1760
67	8.04	100.06	2071.8	0.0110	1765
72	16.22	100.06	2067.6	0.0086	3551
78	16.22	100.06	2063.6	0.0111	3532
76	32.29	100.02	2064.1	0.0121	7032
77	32.26	100.02	2068.8	0.0098	7066

TABLE II. MACROSCOPIC THERMAL TRANSPORT FROM A 0.5-INCH HEATED SPHERE

Test Number	Macroscopic Nusselt Number		$\frac{Nu_1^*}{Re}$	Total Thermal Flux ^a Btu/Sec		Average Surface Temperature OF
	Free Stream	Surface		Observed	Integrated	
63	18.60	15.96	0.537	1.1140×10^{-3}	0.860×10^{-3}	205.4
65	18.62	16.61	0.560	0.7987	0.593	175.6
62	25.72	22.90	0.547	1.1132	0.838	176.3
67	26.05	24.00	0.573	0.7982	0.588	154.0
72	35.69	30.60	0.515	2.1247	1.790	204.9
78	35.11	31.23	0.525	1.5616	1.339	178.4
76	51.41	44.28	0.528	2.9103	2.503	199.7
77	51.14	45.50	0.541	2.1261	1.750	173.2

^a Both total thermal fluxes were corrected for the area of the supporting tubes.

TABLE III. EXPERIMENTAL CONDITIONS IN BOUNDARY LAYER OF A 0.5-INCH HEATED SPHERE

Polar Angle	Radial Wire Temperature Gradient at Surface	Relative Nusselt Number	Local Nusselt Number	Surface Temperature	Wire Temperature at Surface	Thermal Boundary Layer Thickness
Degrees	$^{\circ}\text{F}/\text{ft}$			$^{\circ}\text{F}$	$^{\circ}\text{F}$	ft
Test 63						
0	8.05×10^4	2.58	41.2	204.0	177.2	8.2×10^{-4}
41.3	5.52	1.77	28.3	204.3	179.9	7.8
59.9	4.57	1.46	23.3	204.8	181.8	10.8
75.6	3.66	1.17	18.7	205.2	184.1	13.1
90.0	2.80	0.90	14.4	205.4	186.0	16.7
121.0	1.01	0.32	5.1	205.8	188.8	35.6
168.7	1.74	0.56	8.9	206.0	-	-
Test 65						
0	5.80×10^4	2.59	43.0	174.6	153.7	7.3×10^{-4}
41.3	3.85	1.72	28.6	174.8	157.4	8.6
60.2	3.26	1.46	24.3	175.1	158.6	10.9
75.8	2.70	1.21	20.1	175.4	160.0	13.1
90.0	2.06	0.92	15.3	175.6	161.3	16.0
119.8	0.74	0.33	5.5	175.9	163.6	36.0
166.7	1.19	0.53	8.8	176.0	-	-

TABLE III. (Cont.)

Polar Angle	Radial Wire Temperature Gradient at Surface	Relative Nusselt Number	Local Nusselt Number	Surface Temperature	Wire Temperature at Surface	Thermal Boundary Layer Thickness
Degrees	°F/ft			°F	°F	ft
Test 62						
0	7.30	2.32	53.1	175.0	151.4	5.9×10^{-4}
41.8	6.12	1.94	44.4	175.3	154.3	5.6
66.9	4.48	1.42	32.5	175.8	157.7	7.5
90.0	2.85	0.90	20.6	176.4	161.0	11.6
120.6	0.75	0.24	5.5	176.8	163.9	31.2
161.3	1.01	0.32	7.3	176.8	-	-
Test 67						
0	5.35	2.34	56.2	153.1	136.6	5.1×10^{-4}
41.3	4.27	1.87	44.9	153.3	139.1	5.3
59.9	3.43	1.50	36.0	153.6	140.1	7.4
75.6	2.94	1.29	31.0	153.8	141.9	9.0
90.0	2.02	0.88	21.1	154.1	143.3	11.4
121.0	0.59	0.26	6.2	154.3	145.6	31.2
168.7	1.27	0.55	13.2	154.4	-	-

68

TABLE III. (Cont.)

Polar Angle Degrees	Radial Wire Temperature Gradient at Surface °F/ft	Relative Nusselt Number	Local Nusselt Number	Surface Temperature °F	Wire Temperature at Surface °F	Thermal Boundary Layer Thickness ft
Test 72						
0	11.55	1.78	54.5	203.4	168.5	5.1×10^{-4}
41.3	12.21	1.88	57.5	203.8	172.9	3.7
59.9	10.64	1.64	50.2	204.2	177.1	5.0
75.6	6.91	1.07	32.7	204.7	180.0	6.2
90.0	4.89	0.75	23.0	205.1	183.5	9.7
121.0	2.91	0.45	13.8	205.6	185.8	28.7
170.9	4.03	0.62	19.0	205.8	-	-
Test 78						
0	8.56	1.70	53.1	177.3	151.0	3.9×10^{-4}
41.4	9.02	1.79	55.9	177.6	154.3	3.6
60.3	7.90	1.57	49.0	177.9	157.2	4.8
75.8	5.10	1.01	31.5	178.1	159.5	6.4
90.0	3.80	0.75	23.4	178.6	161.6	8.8
120.0	2.20	0.44	13.7	178.9	163.7	27.2
166.7	4.35	0.86	26.9	179.1	-	-

TABLE III (Cont.)

Polar Angle Degrees	Radial Wire Temperature Gradient at Surface °F/ft	Relative Nusselt Number	Local Nusselt Number	Surface Temperature °F	Wire Temperature at Surface °F	Thermal Boundary Layer Thickness ft
Test 76						
0	13.86	1.52	67.3	199.0	160.6	4.5×10^{-4}
41.3	14.81	1.62	71.7	199.2	164.3	3.1
60.0	14.92	1.64	72.6	199.3	168.8	3.4
75.7	9.22	1.01	44.7	199.4	173.4	4.7
90.0	6.05	0.66	29.2	199.7	177.7	7.3
120.0	5.18	0.57	25.2	200.1	177.9	21.3
171.8	9.62	1.05	46.5	200.5	-	-
Test 77						
0	10.21	1.55	70.5	172.7	143.9	3.9
41.3	11.68	1.76	80.1	172.8	147.4	2.8
60.0	11.10	1.69	76.9	172.9	150.3	3.4
75.6	7.16	1.09	49.6	173.1	153.7	5.0
90.0	4.51	0.69	31.4	173.2	156.7	6.9
120.0	3.82	0.58	26.4	173.5	156.6	21.0
175.4	3.58	0.54	24.6	173.8	151.0	-

TABLE IV. TYPICAL HORIZONTAL TEMPERATURE TRAVERSE DATA FROM TEST 62

Traverse at $x = -0.187$ in. Polar Angle = 41.8°			Traverse at $x = 0.127$ in. Polar Angle = 120.6°		
Horizontal Distance in.	Radial Distance in.	Wire Temperature $^\circ\text{F}$	Horizontal Distance in.	Radial Distance in.	Wire Temperature $^\circ\text{F}$
0(Surface)	0	154.43 ^a	0(Surface)	0	164.00
0.001	0.0007	152.89	0.001	0.0009	163.42
0.002	0.0013	148.96	0.002	0.0017	162.63
0.003	0.0020	144.52	0.003	0.0026	162.14
0.004	0.0027	142.57	0.005	0.0043	160.86
0.005	0.0033	139.10	0.010	0.0086	158.39
0.006	0.0042	135.83	0.015	0.0129	155.72
0.007	0.0049	132.49	0.020	0.0172	153.14
0.009	0.0063	126.15	0.025	0.0215	150.56
0.012	0.0083	118.03	0.030	0.0258	147.27
0.017	0.0118	108.40	0.035	0.0301	143.17
0.027	0.0188	101.19	0.040	0.0344	138.85
0.052	0.0362	100.20	0.045	0.0388	133.71
0.077	0.0535	100.15	0.050	0.0430	127.93
			0.055	0.0473	117.10
			0.060	0.0516	115.87
			0.065	0.0560	110.41
			0.070	0.0603	106.38
			0.075	0.0645	103.37
			0.080	0.0689	101.81
			0.090	0.0775	100.20
			0.100	0.0861	100.15

^a The difference between the air-stream temperature and 100°F , which was 0.15°F during Test 62, was subtracted from all temperature measurements to base all tests on an air-stream temperature of 100°F .

TABLE V. SMOOTHED LOCAL NUSSLETT NUMBERS

Polar Angle Degrees	Free Stream Reynold Number				
	1000	2000	4000	6000	8000
	Surface Nusselt Number				
0	42.5	49.6	58.9	65.9	71.9
30	36.5	47.6	60.2	70.0	79.8
60	29.0	37.8	53.8	66.8	78.4
90	15.4	20.0	25.5	28.7	31.2
120	4.2	8.3	15.8	22.7	28.6
150	6.5	12.0	21.8	30.3	38.2

Part III

THERMAL TRANSFER IN TURBULENT GAS STREAMS. EFFECT OF TURBULENCE
ON LOCAL TRANSPORT FROM SPHERES *

* Part III was submitted on Feb. 19, 1958 to the Journal of Applied Mechanics for publication.

THERMAL TRANSFER IN TURBULENT GAS STREAMS.
EFFECT OF TURBULENCE ON LOCAL TRANSPORT FROM SPHERES

W. W. Short and B. H. Sage

California Institute of Technology
Pasadena, California

INTRODUCTION

Many experimental measurements have been made of the gross convective thermal transport from spheres, and these have been well correlated by McAdams (1) for conditions of turbulent flow. The predictions of Johnstone (2) and measurements of Tang (3) show a divergence from the correlation of McAdams and this may be the result of differences in levels of turbulence.

Studies of local thermal transport from spheres are limited. Cary (4) investigated local thermal transport from a 5-inch iron sphere in an air stream at Reynolds numbers between 4.4×10^4 and 1.5×10^5 . Similar information was obtained by Lautman and Droege (5) for a 9-inch copper sphere in air at Reynolds numbers between 1.3×10^5 and 1.0×10^6 . The work of Lautman and Droege was repeated by Xenakis and co-workers (6) with a 9-inch sphere and with spheres 6 and 12 inches in diameter. Hsu (7) studied the local thermal transport from spheres under conditions of thermal transport and combined thermal and material transport. His work was carried out with two 0.5-inch spheres for Reynolds numbers, based on properties at the interface, between 1500 and 4200 and at a turbulence level of 0.05% root-mean-square longitudinal fluctuation.

The status of the mathematical analysis of heat transfer in the three-dimensional boundary flow encountered at the surface of spheres was recently reviewed by Hsu (7). Sibulkin (8) developed an exact solution of the thermal transfer at the stagnation point of a sphere. Korobkin (9) applied the Karman-Pohlhausen integral method (10) to the prediction of the local thermal transfer. All of the theoretical predictions of local transport available to the authors appear to be subject to limiting assumptions and to represent only an approximation of the behavior in the boundary flow about a sphere.

The present experimental investigation was concerned with rates of local thermal transport from a silver sphere 0.5 inch in diameter. Measurements were made at Reynolds numbers, based on free stream properties, between 900 and 3600. Local transport was determined from the radial temperature gradients encountered within the boundary flow. This investigation constitutes a portion of a study of the effects of the level and scale of turbulence upon thermal and material transport at relatively low Reynolds numbers.

ANALYSIS

In order to present the temperature distribution about a sphere under conditions of forced convection, it is convenient to consider a normalized temperature distribution in the boundary flow (7). This quantity was defined for present purposes as:

$$\Upsilon = \frac{t - t_{\infty}}{t_i^* - t_{\infty}} \quad (1)$$

It should be emphasized that equation 1 is only one simple means of making a first order correlation of the temperature distribution in the boundary flow about the sphere.

For the present study, the Reynolds number was based upon the properties of the free stream as indicated in the following equation:

$$Re_{\infty} = \frac{d U_{\infty}}{\nu_{\infty}} \quad (2)$$

The macroscopic Nusselt number based on the thermal conductivity of air at the surface of the sphere was evaluated from the following expression:

$$Nu_i^* = \frac{\dot{Q} d}{(t_i^* - t_{\infty}) k_i A} \quad (3)$$

In addition the macroscopic Nusselt number based on the free stream properties was determined from:

$$Nu_{\infty}^* = \frac{\dot{Q} d}{(t_i^* - t_{\infty}) k_{\infty} A} \quad (4)$$

The space-average surface temperature, t_i^* , required in equations 1, 3, and 4 was defined by the following equation:

$$t_i^* = \frac{1}{A} \int_0^A t_i dA \quad (5)$$

The local Nusselt number, based on the molecular characteristics of the fluid at the surface, was defined by:

$$Nu_i = \frac{\dot{Q} d}{(t_i - t_{\infty}) k_i} \quad (6)$$

The local thermal flux was established from:

$$\dot{Q} = -k_i \left(\frac{\partial t}{\partial n} \right)_i \quad (7)$$

Because of the nature of the experimental data, the ratio of the local Nusselt number to the macroscopic Nusselt number was found to be more useful than the local Nusselt number defined by equation 6. The following equation for the relative local Nusselt number is derived from equations 3 and 6:

$$\frac{Nu_i}{Nu_i^*} = \frac{(t_i^* - t_{\infty}) k_i^* \dot{Q} A}{(t_i - t_{\infty}) k_i \int_0^A \dot{Q} dA} \quad (8)$$

The relative Nusselt number of equation 8 can be used to advantage to portray the distribution of local transport for several levels of turbulence.

For the purpose of illustrating directly the effect of level of turbulence, a second relative Nusselt number was employed. This quantity

was the ratio of the local Nusselt number to the local Nusselt number at zero level of turbulence for the same polar angle and Reynolds

number: Nu_i / Nu_{i_0}

METHODS AND EQUIPMENT

The temperature distribution in a turbulent air stream near an electrically heated, silver sphere 0.5 inch in diameter was measured experimentally. The investigation was carried out at a free stream temperature of 100° F. at gross velocities between 4 and 16 feet per second. For each of the velocities investigated the level of turbulence was varied between 0.013 and approximately 0.15 root-mean-square longitudinal fluctuation.

The equipment which furnished the air supply has been described in detail (11). The air stream approached the working section in a 12-inch by 12-inch steel duct and was reduced, within a distance of approximately two feet, to a 12-inch by 3-inch jet in which the sphere was suspended. The undisturbed vertical stream emerging upward from the constricted section yielded a transverse level of turbulence of 0.013 (12) and was believed to be approximately isotropic. The flow was substantially constant throughout the greater part of the cross section of the emerging jet. The temperature of the undisturbed air stream was known within 0.1° F. relative to the international platinum scale (11). The velocity of the stream was established within 0.5 per cent and did not vary more than 0.2 per cent during any one investigation.

In order to vary the level of turbulence, a steel plate 0.1875 inch

in thickness with 0.875-inch holes on 1-inch centers was inserted in the air stream at the exit of the jet. Sections of steel duct 3 inches by 12 inches in cross section, in lengths varying between 3 and 12 inches, were added on the downstream side of the perforated plate in order to permit investigation at several distances downstream from the plate. Davis (13,14) made an extensive investigation of the characteristics of the longitudinal and transverse fluctuating velocities downstream from a grid of the same dimensions. His data were employed in the present study to predict the level of turbulence as a function of position in the wake of the grid. The parameter employed in this investigation was the longitudinal level of turbulence expressed as the ratio of the root-mean-square of the longitudinal component of the fluctuating velocity to the average velocity.

The silver sphere employed in this investigation has been described by Hsu (7). It was provided with a resistance heater which covered uniformly the surface of an inner core. Four 0.005-inch diameter thermocouples were imbedded in the surface of the sphere to measure the surface temperature. The sphere was supported by two horizontal stainless steel tubes 0.090 inch in diameter through which the leads for the heater and thermocouples were introduced. Guard heaters were provided to avoid thermal losses along the supporting tubes. Electrical power added to the sphere was known within 0.1 per cent.

A 0.0003-inch platinum, platinum-rhodium thermocouple mounted upon a conventional probe (7) was used to measure the temperature of the air

in the boundary flow. The position of the thermocouple relative to the surface of the sphere was known within 0.001 inch; and the temperature of the thermocouple was determined within 0.02° F. relative to the international platinum scale. Local fluctuations in air temperature outside the wake of the sphere were of the order of 0.05° F. during the course of a given set of measurements.

Because of temperature gradients along the thermocouple wires, the temperature of the air could not be established without making corrections to the temperature measured at the thermocouple junction. However, because of uncertainties in the evaluation of the local thermal transfer coefficients to the wire and the possibility of other corrections not at present understood, no action was taken to modify the measured temperatures. Instead, the measured wire temperatures were used to compute temperature gradient data. All the temperature gradient data were reduced to relative local transport by application of equations 7 and 8. Throughout the remainder of the discussion the term "wire temperature" is used to refer to the temperature as measured at the thermocouple junction.

The gradients of the wire temperature immediately adjacent to the sphere appear to have been established within three per cent. The resulting absolute values of local thermal flux may involve uncertainties of as much as 20 per cent because of the uncertainties in relating the wire temperature to the air temperature. It is believed that the relative values of the local thermal flux, as defined by equation 8, do not involve

uncertainties of more than four per cent. The molecular properties of air used in this work were based upon a set of critically chosen values (15).

EXPERIMENTAL RESULTS

The conditions associated with the investigation of the temperature distribution surrounding the 0.5-inch sphere are set forth in Tables I and II. The experimental data cover a range of Reynolds numbers from 900 to 3600. Values of the macroscopic Nusselt number from a previous study (16) are in good agreement with the present data.

A sample of the experimental data obtained from horizontal temperature traverses, which were made in the boundary layer around the sphere, is presented in Table III. Similar information was obtained for each set of experimental conditions recorded in Table I. Figure 1 illustrates the horizontal temperature traverse data recorded in Table III and the corresponding radial temperature distributions. The radial distances were established from the apparent point of contact with the sphere. The location of the point of contact between the sphere and thermocouple could not be determined with accuracy. The wire temperature continued to rise as the thermocouple was pressed against the sphere. The temperature gradient in the immediate vicinity of the sphere was extrapolated linearly to the highest temperature reached in the traverse, as shown in the figure.

From data similar to those in Table III, values of radial wire temperature gradients were computed for each temperature traverse which

intersected the sphere. It was found that the radial temperature distributions were substantially linear for distances of as much as 0.03 inch from the sphere. The temperature gradients at the surface were smoothed with respect to polar angle, assuming that the temperature distribution and gradients were symmetrical with respect to the axis of flow.

The normalized wire temperature distribution around the sphere for each set of conditions recorded in Table I is given in Table IV. The behavior for a single set of conditions is illustrated in Figure 2. In the wake of the sphere where vortex streets introduced low frequency fluctuations in the temperature and velocity fields, the fluctuations in temperature were of such low frequencies that they were observed on a galvanometer with a natural period of five seconds. These fluctuations made it very difficult to obtain a suitable time-average temperature distribution in the wake of the sphere, and for that reason no detailed investigation of the temperature distribution in the wake was undertaken. Some data obtained at a polar angle of 150 degrees are presented in Table IV. However, the temperature gradients computed for this angle are subject to large uncertainties.

Table IV also records, for every 30 degrees of polar angle, the relative Nusselt number (Nu_i / Nu_i^*); the absolute Nusselt number (Nu_i) computed from equation 8; and the relative Nusselt number (Nu_i / Nu_{i0}). These local dimensionless groups were based on the smoothed temperature gradients. The normalized surface temperatures, included in Table IV,

are from the work of Sato (16).

Figure 3 presents the relative local Nusselt number, Nu_i/Nu_i^* , as a function of polar angle, with the level of longitudinal turbulence as a parameter. The data in this figure are for an average Reynolds number of 3545. It should be emphasized that the Reynolds number was computed from the molecular conditions existing in the free stream, whereas the Nusselt number was computed on the basis of the molecular properties of the air stream at the surface. The velocity, 16.14 feet per second, given in Figures 3, 4, and 5 is the average velocity for the four tests used in those figures.

Figure 3 shows that there is a marked variation in the relative local Nusselt number with polar angle and that the level of turbulence exerts significant influence upon the distribution of local transport from the sphere. It should be noted that while the relative heat transfer at the stagnation point appears to remain constant, the absolute heat transfer at this point increases with turbulence level in the same manner as does the over-all heat transfer. Figure 3 shows an increase in heat transfer with respect to polar angle in the vicinity of the stagnation point. This apparent increase may result from the disturbance in the boundary layer caused by the presence of the thermocouple wire. A study of the problems involved in measuring air temperatures in thin boundary layers is to be presented in a later paper (17).

The data of Figure 3 for relative local Nusselt number, Nu_i/Nu_i^* , were interpolated for even values of turbulence level, and the curves for even

turbulence levels are shown in Figure 4. Also included in Figure 4 are experimental data of Hsu (7) for a turbulence level of 0.052 and the theoretical predictions of Sibulkin (18) and Drake (19). Hsu's measurements are in good agreement with the current data except near stagnation where some divergence between the two sets of measurements is encountered. The present data are based upon much more experimental information and are believed to reflect the influence of turbulence more accurately than the reconnaissance study by Hsu. For the theoretical predictions no consideration was taken of the effect of turbulence so that it is not surprising that some disagreement between experiment and prediction is found.

A clearer indication of the influence of level of turbulence on thermal transport from a sphere is given in Figure 5 by use of the second relative local Nusselt number, Nu_i / Nu_{i0} . This relative Nusselt number is presented as a function of polar angle for several levels of turbulence at a representative velocity of 16.14 feet per second, which corresponds to a Reynolds number of 3545. The local Nusselt number at zero level of turbulence, Nu_{i0} , was obtained by extrapolation of the local Nusselt numbers at four levels of turbulence. Figure 5 demonstrates the large effect of turbulence on the heat transfer in the wake of the sphere.

In conclusion, it may be stated that the use of the Nusselt number as a single-valued function of the Reynolds number for a particular body does not provide an adequate description of the transport characteristics

encountered in turbulent flow. It appears necessary to consider some other factor or factors describing the nature of the turbulent fluctuation in order to obtain a more accurate description of the transport characteristics in the boundary flow. Neither is the use of level of turbulence considered to be a completely satisfactory means of describing the characteristics of turbulence, since it takes into account only the magnitude of the fluctuating velocities and does not portray the scale.

ACKNOWLEDGMENT

The Fluor Corporation contributed to support of the experimental program, and the senior author was the recipient of the Peter E. Fluor Fellowship. The assistance of N. T. Hsu and Kazuhiko Sato in the accumulation of the experimental data is acknowledged. Lorine Faris carried out many of the calculations associated with reduction of the experimental data, and Ann Hansen contributed to preparation of the manuscript.

NOMENCLATURE

A	area, sq. ft.
d	diameter of sphere, in. or ft.
d	differential operator
k	thermal conductivity, Btu/(sq.ft.)(sec.)(°F./ft.)
n	radial or normal distance from surface, in. or ft.
Nu	Nusselt number
\dot{Q}	local thermal flux from surface, Btu/(sec.)(sq.ft.)
\dot{Q}	total thermal flux from surface, Btu/sec.
Re	Reynolds number
t	temperature, °F.
U_{∞}	bulk or free stream velocity, ft./sec.
x, z	coordinate axes with origin at center of sphere, in.
α_T	turbulence level (fractional)
ν	kinematic viscosity, sq.ft./sec.
T	normalized temperature ratio
ψ	polar angle from stagnation point, deg.
∂	partial differential operator

Subscripts

i	solid-gas interface
∞	free stream
0	zero turbulence level

Superscripts

*	space average
---	---------------

LITERATURE CITED

1. "Heat Transmission," by W. H. McAdams, McGraw-Hill Book Company, Inc., New York, N. Y., third edition, 1954.
2. "Heat Transfer to Clouds of Falling Particles," by H. F. Johnstone, R. L. Pigford, and J. H. Chapin, Transactions of the American Institute of Chemical Engineers, vol. 37, 1941, pp. 95-133.
3. "Heat and Momentum Transfer Between a Spherical Particle and Air Streams," by Y. S. Tang, J. M. Duncan, and H. E. Schweyer, NACA Technical Note 2867, March 1953.
4. "The Determination of Local Forced-Convection Coefficients for Spheres," by J. R. Cary, Trans. ASME, vol. 75, 1953, pp. 483-487.
5. "Thermal Conductances about a Sphere Subjected to Forced Convection," by L. G. Lautman and W. C. Droege, Report No. AIRL A 6118 50-15-3, U.S. Air Force, Air Materiel Command, Willow Run Airport, Ypsilanti, Mich., August 1950.
6. "An Investigation of the Heat-Transfer Characteristics of Spheres in Forced Convection," by G. Xenakis, A. E. Amerman, and R. W. Michelson, Technical Report 53-117, Wright Air Development Center, Dayton, Ohio, April 1953.
7. "Thermal and Material Transfer in Turbulent Gas Streams. Local Transport from Spheres," by N. T. Hsu and B. H. Sage, A.I.Ch.E. Journal, vol. 3, 1957, pp. 405-410.
8. "Heat Transfer near the Forward Stagnation Point of a Body of Revolution," by Merwin Sibulkin, Journal of Aeronautical Sciences, vol. 19, 1952, pp. 570-572.
9. "Discussion of Local Laminar Heat Transfer Coefficients for Spheres and Cylinders in Incompressible Flow," by Irving Korobkin, Paper No. 54-F-18-Revised, contributed by the Heat Transfer Division for presentation at the ASME Fall Meeting, Milwaukee, Wisconsin, September 8-10, 1954.
10. "Über laminare und turbulente Reibung," by Th. von Karman, Zeitschrift ang^{ew}andter Mathematik und Mechanik, vol. 1, 1921, pp. 233-252.
11. "Experimental Methods for Measurement of the Evaporation of Drops," by N. T. Hsu, H. H. Reamer, and B. H. Sage, Document No. 4219, American Documentation Institute, Library of Congress, Washington, D. C., 1954.

12. "A Turbulence Indicator Utilizing the Diffusion of Heat," by G. B. Schubauer, NACA Report No. 524, 1935.
13. "Measurements of Turbulence Level behind a set of Square-Mesh Grids and Correlation with Grid Pressure Loss," by Leo Davis, Report 2-22, Jet Propulsion Laboratory, California Institute of Technology, Pasadena, Calif., 1950.
14. "Measurements of Turbulence Decay and Turbulent Spectra behind Grids," by Leo Davis, Report 2-17, Jet Propulsion Laboratory, California Institute of Technology, Pasadena, Calif., 1952.
15. "Thermal and Material Transfer in Turbulent Gas Streams. Local Transport from Spheres," by N. T. Hsu and B. H. Sage, Document No. 5311, American Documentation Institute, Library of Congress, Washington, D. C., 1957.
16. "Thermal Transfer in Turbulent Gas Streams. Effect of Turbulence on Macroscopic Transport from Spheres," by Kazuhiko Sato and B. H. Sage, Paper No. 57-A-29, contributed by the Heat Transfer Division for presentation at the ASME Annual Meeting, New York, N. Y., December 1-6, 1957.
17. "Thermal Transfer in Turbulent Gas Streams. Distribution of Temperature and Thermal Flux around Spheres," by W. W. Short, Kazuhiko Sato, and B. H. Sage, to be submitted to Trans. ASME.
18. "Theoretical Solutions for Heat Transfer on a Sphere," by Merwin Sibulkin, unpublished, 1952.
19. "Calculation Method for Three-Dimensional Rotationally Symmetrical Laminar Boundary Layers with Arbitrary Free-Stream Velocity and Arbitrary Wall-Temperature Variation," by R. M. Drake, Jr., Journal of the Aeronautical Sciences, vol. 20, 1953, pp. 309-316.

LIST OF FIGURES

1. Comparison of Horizontal and Radial Temperature Distributions
2. Wire Temperature Distribution around a 0.5-Inch Heated Sphere
3. Effect of Polar Angle upon Local Nusselt Number Nu_i / Nu_i^*
4. Comparison of Local Transport from Several Investigations
5. Influence of Level of Turbulence upon Thermal Transport

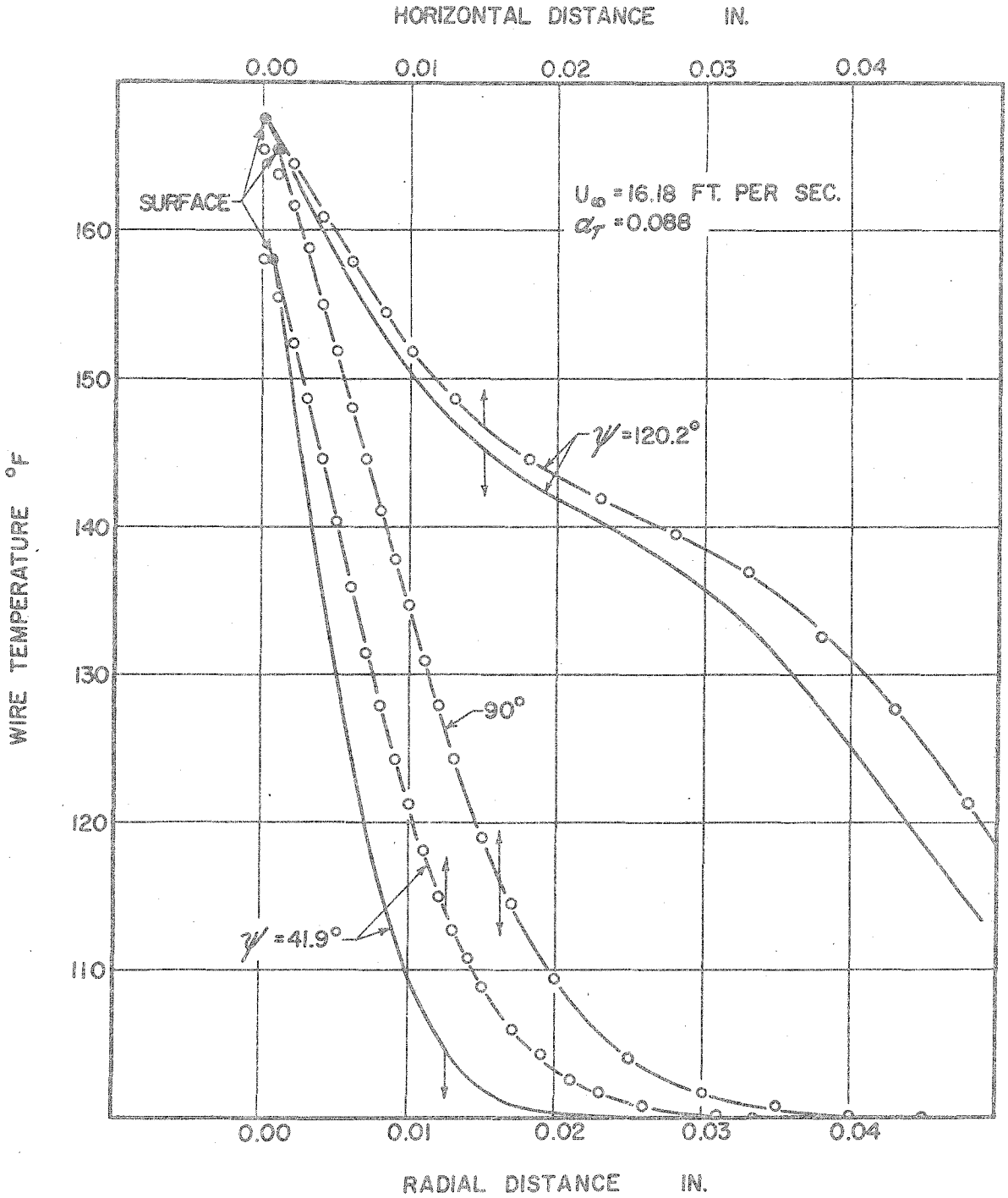


Fig. 1. Comparison of Horizontal and Radial Temperature Distributions

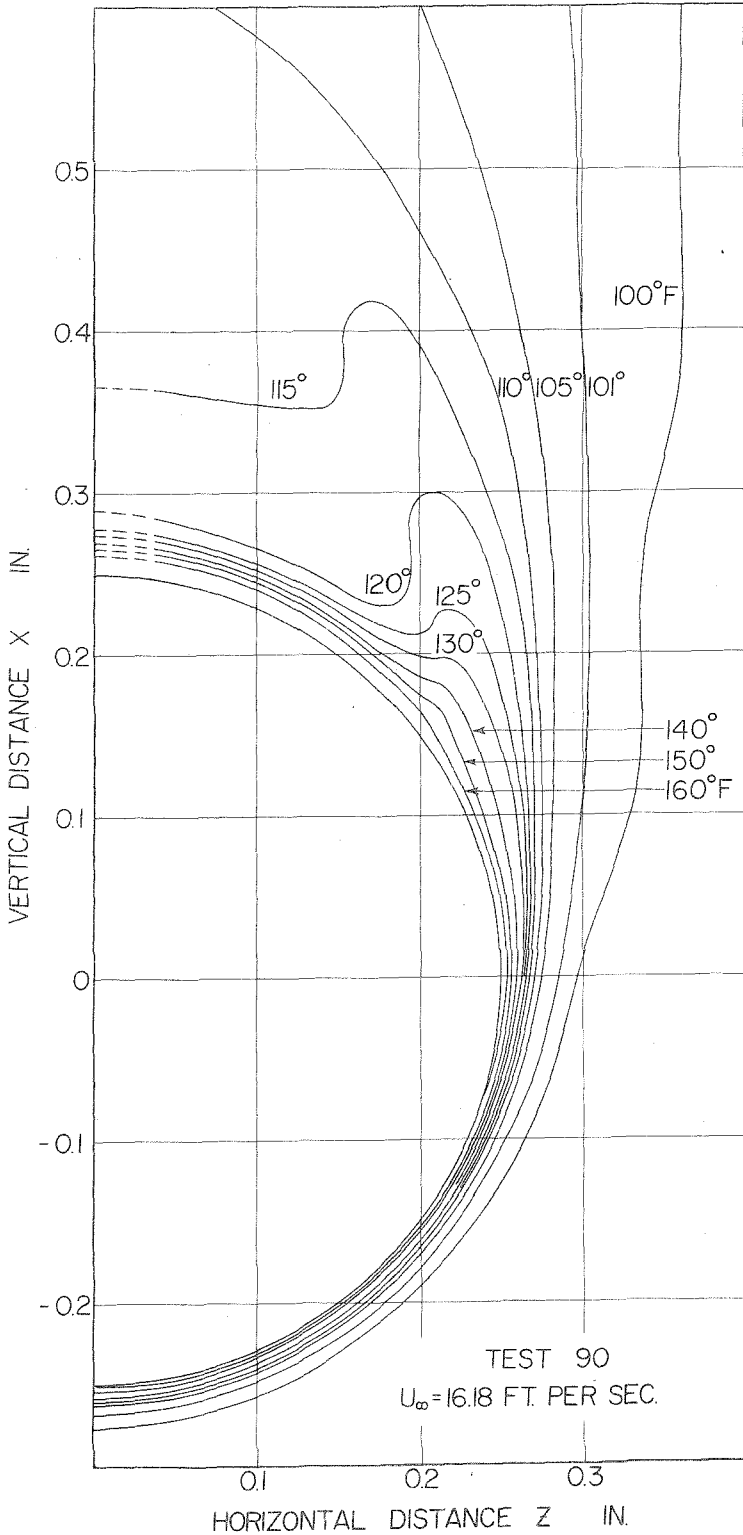


Fig. 2. Wire Temperature Distribution around a 0.5-inch Heated Sphere

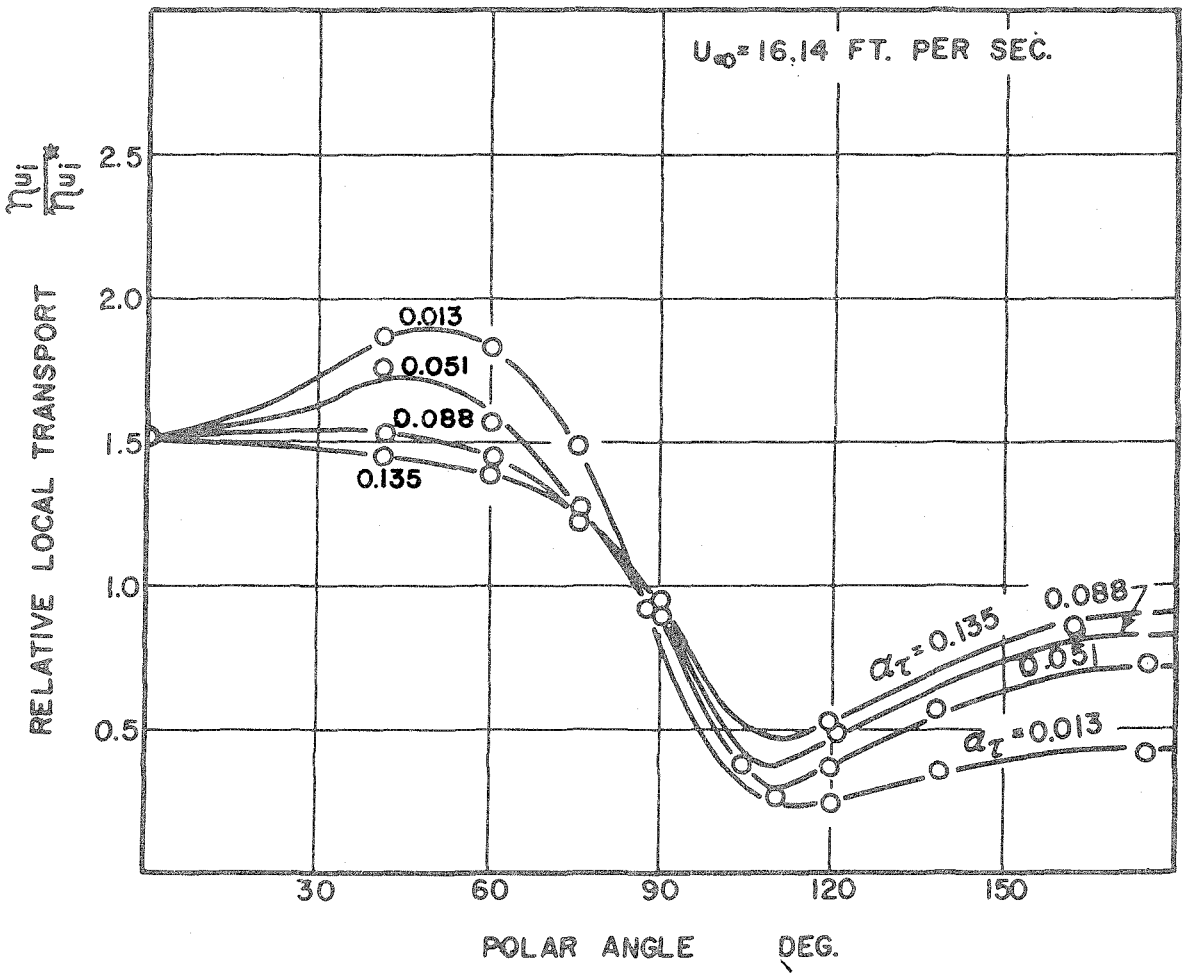


Fig. 3. Effect of Polar Angle upon Local Nusselt Number $\frac{Nu_i}{Nu_i^*}$

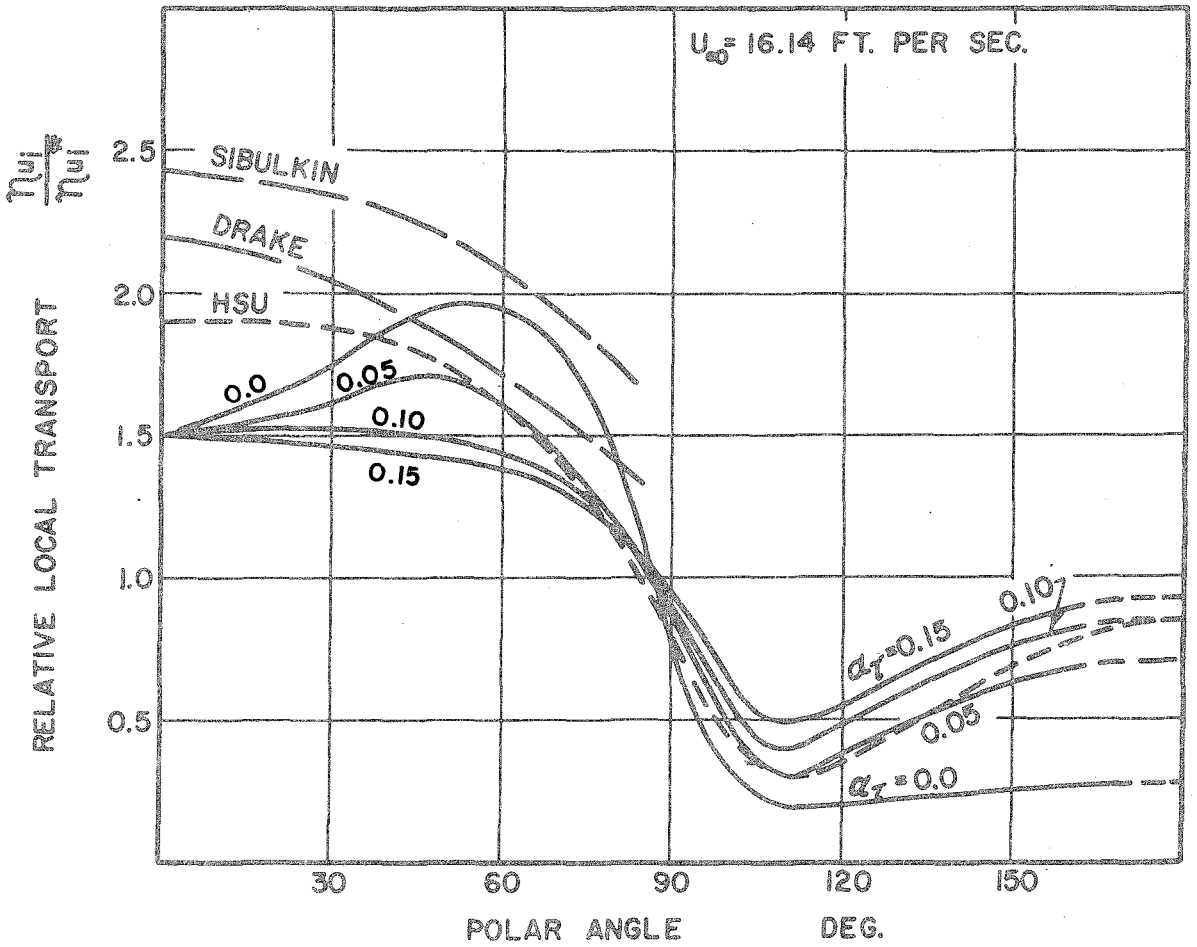


Fig. 4. Comparison of Local Transport from Several Investigations

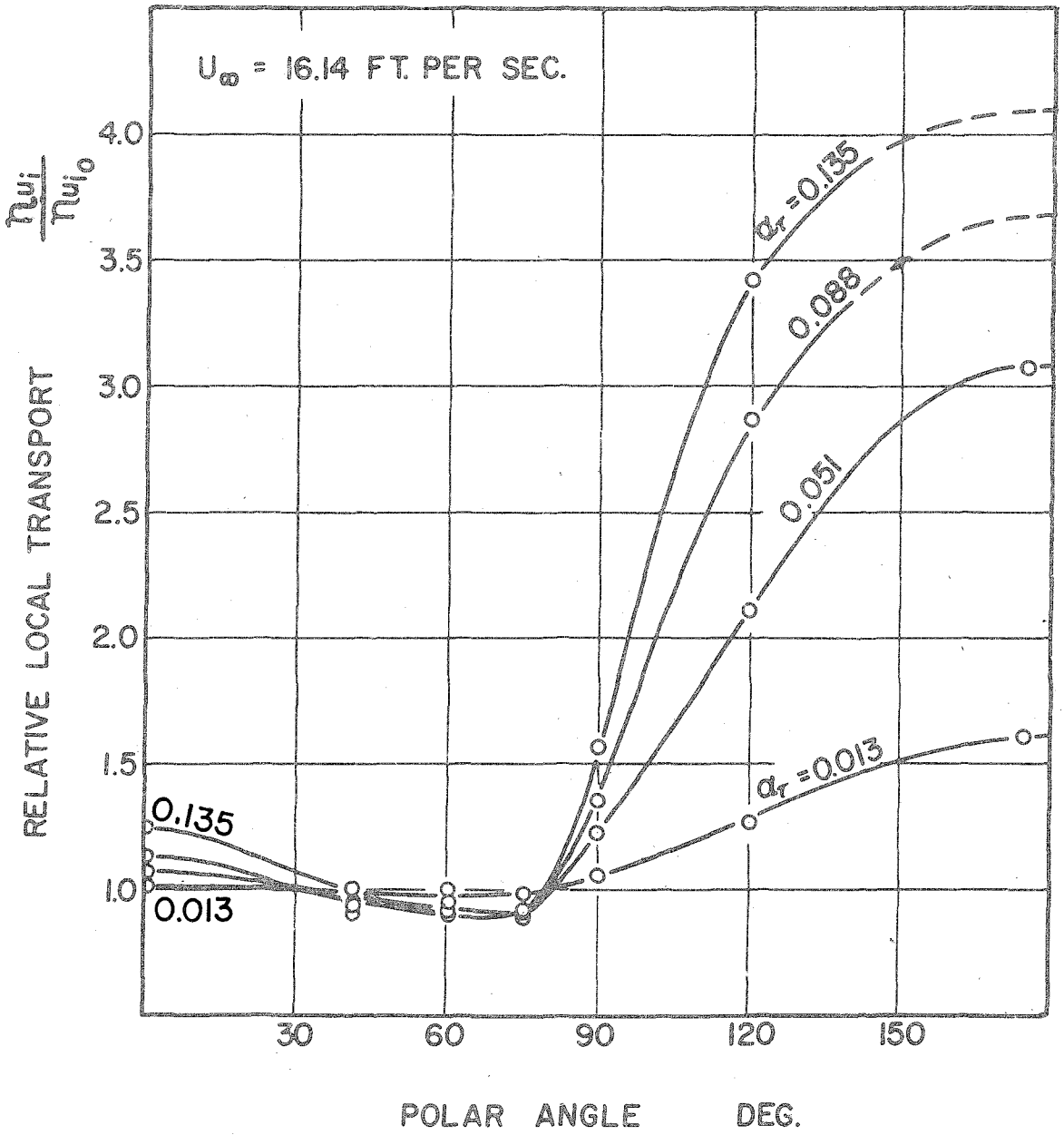


Fig. 5. Influence of Level of Turbulence upon Thermal Transport

LIST OF TABLES

- I. Experimental Conditions in Air Stream
- II. Thermal Transport from a 0.5-Inch Heated Sphere
- III. Typical Horizontal Temperature Traverse Data from Test 90
- IV. Local Conditions around the Sphere

TABLE I. EXPERIMENTAL CONDITIONS IN AIR STREAM

Test Number	Velocity ft./sec.	Level of Turbulenced Fraction	Temperature of.	Pressure lb./sq.ft. Absolute	Weight Fraction Water
161	4.03	0.013	100.13	2068.6	0.0122
110	8.06	0.054	100.06	2055.9	0.0048
89	8.04	0.094	100.06	2064.1	0.0052
92	7.98	0.146	100.06	2080.8	0.0060
93	8.01	0.146	100.03	2073.6	0.0060
160	16.14	0.013	100.06	2066.1	0.0091
109	16.13	0.051	100.06	2069.2	0.0035
90	16.18	0.088	100.06	2067.2	0.0053
91	16.09	0.135	100.06	2077.8	0.0051

^a Longitudinal level of turbulence expressed as the ratio of the root-mean-square of the longitudinal component of the fluctuating velocity to the average velocity.

TABLE II. THERMAL TRANSPORT FROM A 0.5-INCH HEATED SPHERE

Test Number	Reynolds Number Free Stream	Macroscopic Nusselt Number Free Stream	Surface	Average Surface Temperature of.	Total Thermal Flux Experimental Btu/sec
161	882	18.23	16.26	177.0	0.7972×10^{-3}
110	1749	25.99	23.30	175.5	1.1146
89	1758	26.01	23.17	175.4	1.1146
92	1772	27.44	24.68	171.5	1.1146
93	1768	27.59	24.82	171.1	1.1148
160	3527	36.98	30.00	206.0	2.1247
109	3548	36.53	32.67	175.2	1.5617
90	3548	37.44	33.35	173.4	1.5616
91	3565	40.94	36.95	167.1	1.5621

^a The total observed energy addition was corrected for the area of the supporting tubes.

TABLE III. TYPICAL HORIZONTAL TEMPERATURE TRAVERSE DATA FROM TEST 90

Horizontal traverse at $x = -0.186$ inch ($\psi = 41.9^\circ$)			Horizontal Traverse at $x = 0.001$ inch ($\psi = 90^\circ$)		
Horizontal Distance in.	Radial Distance in.	Wire Temperature OF	Horizontal Distance in.	Radial Distance in.	Wire Temperature OF.
0	0	158.31	0	0	165.43
0.001	0.0005	155.66	0.001	0.001	163.85
0.002	0.0015	152.46	0.002	0.002	161.75
0.003	0.0020	148.70	0.003	0.003	158.84
0.004	0.0026	144.66	0.004	0.004	155.12
0.005	0.0033	140.32	0.005	0.005	151.92
0.006	0.0040	135.95	0.006	0.006	148.16
0.007	0.0045	131.55	0.007	0.007	144.66
0.008	0.0051	127.96	0.008	0.008	141.14
0.009	0.0062	124.35	0.009	0.009	137.86
0.010	0.0068	121.28	0.010	0.010	134.58
0.011	0.0075	118.19	0.011	0.011	131.00
0.012	0.0082	115.10	0.012	0.012	127.96
0.013	0.0088	112.84	0.013	0.013	124.35
0.014	0.0095	110.86	0.015	0.015	119.04
0.015	0.0102	108.86	0.017	0.017	114.54
0.017	0.0115	106.01	0.020	0.020	109.43
0.019	0.0130	104.30	0.025	0.025	104.02
0.021	0.0145	102.58	0.030	0.030	101.72
0.023	0.0160	101.72	0.035	0.035	100.86
0.026	0.0180	100.86	0.040	0.040	100.29
0.031	0.0217	100.29	0.045	0.045	100.00
0.036	0.0254	100.00			

TABLE III. (Cont.)

Horizontal Traverse
at $x = 0.126$ inch ($\psi = 120.20$)

Horizontal Distance in.	Radial Distance in.	Wire Temperature of
0	0	167.52
0.002	0.0018	164.64
0.004	0.0035	160.96
0.006	0.0050	158.05
0.008	0.0070	154.86
0.010	0.0088	151.92
0.013	0.0114	148.70
0.018	0.0158	144.66
0.023	0.0201	141.95
0.028	0.0246	139.50
0.033	0.0290	137.04
0.038	0.0335	132.65
0.043	0.0380	127.68
0.048	0.0425	121.28
0.053	0.0472	115.94
0.058	0.0515	110.86
0.063	0.0561	107.15
0.068	0.0607	104.02
0.078	0.0698	101.15
0.093	0.0836	100.29
0.118	0.1096	100.00

TABLE IV. LOCAL CONDITIONS AROUND THE SPHERE - TEST 161

Polar Angle	0°	30°	60°	90°	120°	150°
Nu_i / Nu_i^*	1.83 ^a	1.90	1.56	0.85	0.34	0.59
Nu_i	29.8 ^b	30.9	25.4	13.8	5.5	9.6
Nu_i / Nu_{i0}	c	-	-	-	-	-
Normalized Surface Temp.	0.987	0.989	0.994	1.000	1.004	1.006
Radial Distance from Surface, in.	Normalized Wire Temperature					
0	0.845	0.854	0.882	0.922	0.951	
0.005	0.607	0.760	0.713	0.818	0.900	
0.010	0.362	0.397	0.542	0.716	0.854	
0.015	0.181	-	0.369	-	0.818	
0.020	-	-	0.195	-	0.786	
0.025	-	-	-	-	0.755	
0.030	-	-	-	-	0.723	
0.040	-	-	-	-	0.653	
0.050	-	-	-	-	0.553	
0.060	-	-	-	-	-	
0.080	-	-	-	-	-	
0.100	-	-	-	-	-	
0.150	-	-	-	-	-	
0.200	-	-	-	-	-	
0.250	-	-	-	-	-	
0.300	-	-	-	-	-	

^a Values of Nu_i / Nu_i^* obtained from equation 8.

^b Values of Nu_i obtained from values of Nu_i / Nu_i^* and the experimental values of surface Nusselt number, Nu_i^* , in Table II.

^c Nu_i could not be extrapolated to zero turbulence level at 4 ft/sec because of insufficient data at this velocity.

TABLE IV. (Cont.) - TEST 110

Polar Angle	0°	30°	60°	90°	120°	150°
Nu_i / Nu_i^*	1.63	1.71	1.64	0.95	0.25	0.60
Nu_i	38.0	39.8	38.2	22.1	5.8	14.0
Nu_i / Nu_{i0}	1.01	1.00	0.98	0.97	1.06	1.11
Normalized Surface Temp.	0.983	0.985	0.992	1.001	1.006	1.007
Radial Distance from Surface, in.	Normalized Wire Temperature					
0	0.814	0.829	0.862	0.903	0.927	0.937
0.005	0.525	0.548	0.588	0.736	0.880	0.844
0.010	0.240	0.260	0.312	0.570	0.831	0.751
0.015	0.0829	0.0643	0.133	0.401	0.783	0.661
0.020	0.0218	0.00610	0.0371	0.233	0.734	0.586
0.025	0.00398	0.000	0.00663	0.110	0.682	0.519
0.030	0.000	-	0.000	0.0497	0.625	0.476
0.040	-	-	-	0.0590	0.486	0.442
0.050	-	-	-	0.000	0.345	0.430
0.060	-	-	-	-	0.208	0.423
0.080	-	-	-	-	0.478	0.424
0.100	-	-	-	-	0.00265	0.434
0.150	-	-	-	-	0.000	0.369
0.200	-	-	-	-	-	0.167
0.250	-	-	-	-	-	0.424
0.300	-	-	-	-	-	0.00597

TABLE IV. (Cont.) - TEST 89

Polar Angle	0°	30°	60°	90°	120°	150°
Nu_i/Nu_i^*	1.63	1.67	1.60	0.92	0.30	0.65
Nu_i	37.8	38.7	37.7	21.3	6.9	15.1
Nu_i/Nu_{i0}	1.03	1.00	0.96	0.96	1.16	1.29
Normalized Surface Temp.	0.983	0.985	0.992	1.001	1.006	1.007
Radial Distance from Surface, in.	Normalized Wire Temperature					
0	0.758	0.783	0.835	0.881	0.901	0.909
0.005	0.470	0.459	0.531	0.707	0.838	0.816
0.010	0.214	0.164	0.254	0.536	0.775	0.723
0.015	0.0750	0.0531	0.173	0.360	0.713	0.634
0.020	0.0226	0.0106	0.0438	0.218	0.651	0.545
0.025	0.00318	0	0.0133	0.114	0.589	0.476
0.030	0	-	0.0265	0.0617	0.527	0.435
0.040	-	-	0	0.0154	0.403	0.388
0.050	-	-	-	0.00133	0.289	0.358
0.060	-	-	-	0	0.186	0.339
0.080	-	-	-	-	0.0541	0.330
0.100	-	-	-	-	0.00796	0.340
0.150	-	-	-	-	0	0.301
0.200	-	-	-	-	-	0.177
0.250	-	-	-	-	-	0.0727
0.300	-	-	-	-	-	0.0252

TABLE IV. (Cont.) - TEST 92

Polar Angle	0°	30°	60°	90°	120°	150°
Nu_i/Nu_i^*	1.63	1.67	1.60	0.92	0.30	0.65
Nu_i	40.5	40.2	38.0	21.7	9.1	20.6
Nu_i/Nu_{i0}	1.03	1.00	0.96	0.96	1.16	1.29
Normalized Surface Temp.	0.983	0.985	0.992	1.001	1.006	1.007
Radial Distance from Surface, In.	Normalized Wire Temperature					
0	0.805	0.824	0.856	0.887	0.908	0.914
0.005	0.506	0.560	0.610	0.707	0.845	0.802
0.010	0.210	0.293	0.364	0.524	0.780	0.651
0.015	0.0693	0.105	0.161	0.342	0.715	0.515
0.020	0.0336	0.0483	0.0791	0.210	0.649	0.374
0.025	0.0168	0.021	0.0448	0.128	0.587	0.300
0.030	0.00770	0.00880	0.0258	0.0833	0.522	0.277
0.040	0	0.00140	0.0154	0.0385	0.405	0.252
0.050	-	0	0.00210	0.0175	0.309	0.237
0.060	-	-	0	0.0840	0.235	0.228
0.080	-	-	-	0.00252	0.118	0.214
0.100	-	-	-	0	0.0280	0.206
0.150	-	-	-	-	0.0077	0.188
0.200	-	-	-	-	0	0.156
0.250	-	-	-	-	-	0.104
0.300	-	-	-	-	-	0.0630

TABLE IV. (Cont.) - TEST 93

Polar Angle	0°	30°	60°	90°	120°	150°
Nu_i/Nu_i^*	1.63	1.62	1.53	0.88	0.37	0.83
Nu_i	40.5	40.2	38.0	21.7	9.1	20.6
Nu_i/Nu_{i0}	1.09	1.06	1.00	0.96	1.30	1.68
Normalized Surface Temp.	0.983	0.985	0.992	1.001	-	-
Radial Distance from Surface, In.	Normalized Wire Temperature					
0	0.805	0.824	0.856	0.887	0.908	0.914
0.005	0.476	0.563	0.590	0.711	0.847	0.759
0.010	0.170	0.305	0.331	0.540	0.783	0.598
0.015	0.0704	0.101	0.120	0.369	0.719	0.436
0.020	0.0345	0.0450	0.0633	0.200	0.656	0.322
0.025	0.016	0.0211	0.0373	0.115	0.591	0.289
0.030	0.00591	0.00844	0.0239	0.0753	0.527	0.269
0.040	0	0.00141	0.0985	0.0373	0.407	0.247
0.050	-	0	0.0281	0.0194	0.308	0.240
0.060	-	-	0	0.0101	0.231	0.236
0.080	-	-	-	0.00310	0.115	0.231
0.100	-	-	-	0	0.0549	0.228
0.150	-	-	-	-	0.00732	0.209
0.200	-	-	-	-	0	0.158
0.250	-	-	-	-	-	0.103
0.300	-	-	-	-	-	0.0640

TABLE IV. (Cont.) - TEST 160

Polar Angle	0°	30°	60°	90°	120°	150°
Nu_i / Nu_i^*	1.51	1.72	1.83	0.80	0.25	0.39
Nu_i	47.1	53.5	54.3	24.0	7.5	11.7
Nu_i / Nu_{i0}	1.01	0.99	0.98	1.06	1.29	1.51
Normalized Surface Temp.	0.986	0.988	0.993	1.002	1.007	1.008

Radial Distance from Surface, in.

Normalized Wire Temperature

0	0.924	0.927	0.918	0.943	0.976	
0.005	0.831	0.585	0.499	-	0.839	
0.010	0.727	0.237	0.174	-	0.778	
0.015	0.624	0.053	0.0366	-	0.737	
0.020	0.521	-	-	-	0.698	
0.025	0.417	-	-	-	0.663	
0.030	-	-	-	-	0.627	
0.040	-	-	-	-	0.548	
0.050	-	-	-	-	0.420	
0.060	-	-	-	-	0.164	
0.080	-	-	-	-	0.0479	
0.100	-	-	-	-	0.0103	
0.150	-	-	-	-	-	
0.200	-	-	-	-	-	
0.250	-	-	-	-	-	
0.300	-	-	-	-	-	

TABLE IV. (Cont.) - TEST 109

Polar Angle	0°	30°	60°	90°	120°	150°
Nu_i / Nu_j^*	1.51	1.64	1.61	0.88	0.38	0.63
Nu_i	49.0	53.2	53.1	28.1	12.4	20.6
Nu_i / Nu_{i0}	1.08	0.98	0.93	1.23	2.14	2.87
Normalized Surface Temp.	0.966	0.988	0.993	1.002	1.007	1.008

Radial Distance from Surface, in.

Normalized Wire Temperature

0	0.837	0.851	0.880	0.917	0.939	0.956
0.005	0.432	0.389	0.496	0.677	0.844	0.778
0.010	0.0891	0.0652	0.162	0.441	0.760	0.605
0.015	0.0193	0.00825	0.0279	0.214	0.713	0.455
0.020	0.00293	0	0.00466	0.0805	0.678	0.391
0.025	0	-	0	0.0239	0.644	0.353
0.030	-	-	-	0.00466	0.607	0.326
0.040	-	-	-	0	0.521	0.287
0.050	-	-	-	-	0.356	0.263
0.060	-	-	-	-	0.174	0.252
0.080	-	-	-	-	0.0705	0.234
0.100	-	-	-	-	0.0220	0.238
0.150	-	-	-	-	0.0479	0.291
0.200	-	-	-	-	0	0.183
0.250	-	-	-	-	-	0.0479
0.300	-	-	-	-	-	0.00825

TABLE IV. (Cont.) - TEST 90

Polar Angle	0°	30°	60°	90°	120°	150°
Nu_i / Nu_i^*	1.51	1.54	1.45	0.92	0.46	0.74
Nu_i	50.6	53.0	51.9	31.4	15.3	24.7
Nu_i / Nu_{i0}	1.14	0.99	0.90	1.38	2.84	3.49
Normalized Surface Temp.	0.986	0.988	0.993	1.002	1.007	1.008
Radial Distance from Surface, in.	Normalized Wire Temperature					
0	0.767	0.791	0.846	0.887	0.914	0.930
0.005	0.439	0.438	0.490	0.690	0.896	0.832
0.010	0.130	0.106	0.146	0.495	0.725	0.730
0.015	0.0220	0.0252	0.0402	0.303	0.639	0.623
0.020	0.00682	0.00341	0.0102	0.136	0.574	0.518
0.025	0	0.00136	0.00204	0.0689	0.520	0.410
0.030	-	0	0	0.0344	0.466	0.303
0.040	-	-	-	0.0136	0.385	0.261
0.050	-	-	-	0	0.293	0.246
0.060	-	-	-	-	0.200	0.238
0.080	-	-	-	-	0.0552	0.228
0.100	-	-	-	-	0.0286	0.224
0.150	-	-	-	-	0.0136	0.218
0.200	-	-	-	-	0	0.0777
0.250	-	-	-	-	-	0.0348
0.300	-	-	-	-	-	-

TABLE IV. (Cont.) - TEST 91

Polar Angle	0°	30°	60°	90°	120°	150°
Nu_i / Nu_i^*	0.51	1.47	1.39	0.96	0.52	0.80
Nu_i	52.9	52.4	50.4	35.3	19.2	29.6
Nu_i / Nu_{i0}	1.24	1.06	0.91	1.57	3.44	3.96
Normalized Surface Temp.	0.986	0.988	0.993	1.002	1.007	1.008
Radial Distance from Surface, in.	Normalized Wire Temperature					
0	0.761	0.781	0.822	0.861	0.895	0.907
0.005	0.473	0.487	0.542	0.602	0.767	0.754
0.010	0.160	0.197	0.271	0.359	0.661	0.581
0.015	0.0529	0.0686	0.0902	0.230	0.583	0.402
0.020	0.0218	0.0343	0.0423	0.111	0.517	0.257
0.025	0.00745	0.0164	0.0171	0.0641	0.458	0.224
0.030	0	0.00596	0.00745	0.0388	0.406	0.203
0.040	-	0	0	0.0171	0.315	0.184
0.050	-	-	-	0.00820	0.238	0.174
0.060	-	-	-	0.00298	0.175	0.168
0.080	-	-	-	0	0.0868	0.161
0.100	-	-	-	-	0.0343	0.158
0.150	-	-	-	-	0.00596	0.146
0.200	-	-	-	-	0	0.116
0.250	-	-	-	-	-	0.0812
0.300	-	-	-	-	-	0.0522

PROPOSITIONS

1. The thermal boundary layer measured on a sphere exhibited a minimum thickness at approximately 40 degrees from the stagnation point. A rigorous mathematical treatment of the flow in this region is proposed to determine whether this is a general property of the flow or a result of the particular equipment used.
2. An anemometer having a small heat capacity or a thermocouple having a small conduction correction can be made by condensing metals at low pressure on a quartz fiber.
3. A theoretical study of energy transfer from a fluid to a solid surface which has a radius of curvature small compared to the mean free path of the fluid may prove interesting.
4. It is difficult to obtain both good heat transfer and durability in rigid fuel elements for a fission reactor. In the absence of a soluble compound of uranium with a small thermal neutron cross section, the fuel might be easily handled as an emulsion or a fluidized bed.
5. There is a need for dense phosphors for scintillation counters. Metal-organic compounds similar to the present organic crystals used may provide such a phosphor.
6. A simple scheme for the analysis of a single sample from the NO_2 - HNO_3 - H_2O system for its three components can be developed.
7. E. R. Parker (1) discovered that freshly prepared crystals of MgO are ductile but become brittle within a few minutes. This embrittlement was attributed to impurities in the crystal. Transition to a different allomorphic form may occur in this manner with the observed results.
8. Certain mixtures of cryolite, fluorite and aluminum fluoride melt at 675°C . The use of such an electrolyte in the Hall cell would permit operating temperatures well below the present 1000°C . This would substantially reduce the cost of aluminum production.
9. A magnetic amplifier is proposed for use in the Chemical Engineering Laboratory to control the input to heaters in place of the thyatron circuits presently used.
10. In order to aid centering of stock in a four-jaw chuck on a lathe, a scale should be etched on each jaw.
11. The chief benefit obtained from the assortment of waxes sold to skiers is psychological. The wax does prevent wetting of the running surface;

however, the low friction between the ski and snow is a result of the water film produced by the high pressure exerted by the ski on the tips of small ice crystals.

12. A sailor on a ship that is close-hauled cannot always tell from the sea and wind on which tack the greatest progress is made. A simple analog computer might be set up using a taffrail log and an anemometer to indicate the velocity component to windward.

Reference

1. Parker, E. R., Scientific American, April 1958.